FIRE AND SAFETY
FIRE SAFE TRANSPORT

Investigation of extinguishing water and combustion gases from vehicle fires

Jonna Hynynen, Ola Willstrand, Per Blomqvist, Maria Quant

RISE Report 2023:22

Abstract

Sales of electric vehicles doubled in 2021 compared to the previous year and nearly 10% of the global new-car sales were electric in 2021. In the recent IEA Global EV Outlook 2022, Norway, Iceland, and Sweden were reported to have the highest electric car shares of the new car market: 86%, 72% and 43%, respectively. Electrification of transport has multiple benefits but has also raised some concerns. For example, the use of rare metals and their sourcing are concerns from an environmental perspective, the capacity of the electricity network and the limited number of charging stations has been raised as an implementation barrier, and the new fire and explosion risks of batteries have caused concerns amongst users, property owners and rescue services alike society.

Fires starting in the traction batteries (lithium-ion battery) are rare but if the battery catches fire, it can be difficult to extinguish since the battery packs are generally well protected and difficult to reach. To cool the battery cells, firefighters must prolong the application duration of suppression agent. This generally results in use of large amounts of water/fire extinguishing agent, which could carry pollutants into the environment.

In this work, extinguishing water from three vehicle fires as well as from one battery pack fire has been investigated. Large-scale fire tests were performed with both conventional and electric vehicles. Tests were performed indoors at RISE, Borås, which also allowed analysis of combustion gases for both inorganic and organic pollutants in the gas and liquid phase.

It was found that nickel, cobalt, lithium, manganese and hydrogen fluoride appeared in higher concentrations in the effluents from the battery electric vehicle and lithium-ion battery compared to from the internal combustion engine vehicle. However, lead was found in higher concentrations in the effluents from the internal combustion engine vehicle, both in the combustion gases as well as in the extinguishing water. Ecotoxicity analysis showed that extinguishing water from all vehicle and battery fires analysed in this work were toxic against the tested aquatic species.

Key words: electric vehicle, battery, fire test, extinguishing water, ecotoxicity

RISE Research Institutes of Sweden AB

RISE Report 2023:22
ISBN: 978-91-89757-65-3
2023

Content

Abstract 1
Content 2
Preface 4
Summary 5
1 Introduction 6
1.1 Lithium-Ion Batteries 6
1.2 Substances Found in Vehicle Fires 8
1.3 Fluorinated Compounds Found in LIBs 9
1.4 Environmental Consequences of Vehicle Fires 11
2 Methods 15
2.1 Fire Tests 15
2.1.1 Test Objects 15
2.1.2 Test Setup 16
2.1.3 Sprinkler System 16
2.2 Analysis methods 18
2.2.1 Heat Release Rate 18
2.2.2 Temperature 18
2.2.3 Gas Analysis 18
2.2.4 Soot Analysis 19
2.2.5 Extinguishing Water Sampling and Analysis 20
2.2.6 Biological Characterisation of Extinguishing Water 21
3 Results and Discussion 22
3.1 Heat Release Rate 23
3.1.1 HRR Reference Test 23
3.1.2 HRR ICEV Test 24
3.1.3 HRR BEV Test 24
3.1.4 HRR Battery Test 25
3.2 Temperature Measurements 25
3.3 Gas Analysis 26
3.3.1 Total Amount of HX from Gas Measurements 27
3.3.2 Soot Analysis 30
3.4 Extinguishing Water Analysis 31
3.4.1 Analysis of Inorganics 31
3.4.2 Analysis of PFAS 33
3.4.3 Analysis of PAHs and VOCs 34
3.4.4 Biological Characterisation 34

4 Conclusions..... 36
References 37
Appendix 1: Fluorinated compounds found in LIBs..... 42
Appendix 2: Gas temperature graphs 43
Appendix 3: Gas analysis - FTIR spectroscopy..... 44
Appendix 4: Soot analysis..... 46
Appendix 5: Water sampling of metals and ions..... 47
Appendix 6: PAH, VOC and PFAS 49

Preface

This work is a continuation of the RISE project ETOX, results presented in RISE report 2020:90 [1] “Toxic Gases from Fire in Electrical Vehicles” funded by the Swedish Energy Agency (No. 48193-1). Results from ETOX provided a scientific basis for relevant risk assessment dealing with fires in electric vehicles. The results regarding the fire extinguishing water analysis presented in this report has previously been published in *Environmental Science and Technology* (DOI: 10.1021/acs.est.2c08581).

The aim of this work is to further address the potential environmental impact of electric vehicle fires. Three large-scale fire tests, using electric and conventional vehicles, as well as a separate lithium-ion battery pack was performed. Additionally, water which is the most common suppression media, has been added in this work using a sprinkler system. Extinguishing water was analysed for both organic and inorganic compounds. Furthermore, ecotoxicity assessment was performed on the extinguishing water.

This work is part of a project (No. 48193-2) financed by the Swedish Energy Agency. Partners within the project: The Swedish Civil Contingencies Agency (MSB), If Skadeförsäkring, Länsförsäkringar Älvsborg, Länsförsäkringar Göteborg & Bohuslän, Stena Teknik, ColdCut systems, Borås Bildemontering and the following fire and rescue services: Räddningstjänsten Storgöteborg, Södra Älvsborgs Räddningstjänstförbund, Storstockholms brandförsvar, Södertörns brandförsvarsförbund, Räddningstjänsten Luleå and Räddningstjänsten Syd.

Acknowledgement

We would like to thank all our colleagues at RISE for their expertise and hard work during the project: Anders Älvskog, Andreas Herbertsson, Anna Sandinge, Christoffer Rapp, Emil Norberg, Eva Emanuelsson, Eskil Sahlin, Fanny Bjarnemark, Henrik Persson, Joel Blom, Lars Gustavsson, Magnus Arvidson, Magnus Viktorsson, Michael Magnusson, Peter Lindqvist, Petra Andersson, Richard Sott, Roeland Bisschop, Sven Karlsson, Sven-Gunnar Gustafsson, Tobias Guldbrand, Tove Mallin and Örjan Westlund. AK Lab and Toxicon AB are acknowledge for the HPIC and the biological characterisation, respectively. Additionally, we would like to thank the car manufacturer for supplying the vehicles used for testing.

Summary

Misconceptions related to fires in electric vehicles may challenge the widespread adoption of electric vehicles and as a result also hinder the required transition from fossil to renewable fuels. In previous work by RISE *Toxic gases from fire in electric vehicles* [1] there was a strong focus on the toxic gases formed upon combustion of conventional and electric vehicles. In this work, the focus is on the extinguishing water resulting from suppression of fires for both battery electric and conventional vehicles.

The aim of this project is to provide a foundation that can be used for relevant risk assessments regarding fires in battery electric vehicles. A literature search, large-scale vehicle fire tests and one battery pack fire test were performed at RISE, Borås. The obtained knowledge will hopefully support the fire and rescue services to execute effective firefighting tactics and provide further insight into how the chosen tactic may affect the environment.

Three large-scale vehicle fire tests and one test with only a battery were performed. Vehicles used for the fire tests included one battery electric vehicle (BEV), one conventional internal combustion engine vehicle (ICEV) and one vehicle where the traction battery had been removed. The vehicle without energy storage was used in a free burning test without addition of water (reference test), the remaining tests were performed having a sprinkler system active. All vehicles were of the same vehicle model, from the same manufacturer, and manufactured in the same year, which enables good direct comparison between the vehicles.

Results obtained regarding the toxic gases analysed, both from vehicle tests and battery test, are consistent with previous work. However, the addition of water from the sprinkler system seems to lower the total concentration of organic and inorganic substances in the gas phase compared to free burning tests.

Metals such as nickel, cobalt, lithium and manganese, together with fluoride was found in higher concentrations in the extinguishing water from the BEV compared to the ICEV. However, lead, volatile organic compounds (VOCs) and polycyclic aromatic hydrocarbons (PAHs) was found in higher concentrations for the ICEV. Additionally, the biological characterisation of the extinguishing water indicated that all tested water samples were toxic towards the tested aquatic species. These results are in coherence with previous work performed by RISE on extinguishing water from ICEVs. [2]

Regarding the overall environmental impact, a range of factors will affect the severeness of pollution. Therefore, it is important to keep in mind that each scenario needs to be assessed individually and that the work performed in this report only represent a small number of samples.

1 Introduction

To ensure continuous safe engineering and development of battery electric vehicles (BEVs), fire testing of batteries and vehicles is still necessary. Fire tests provide data which are essential to fire and rescue services, to enable safe firefighting and rescue tactics for these relatively new energy carriers. Examples of data needed are the heat release rate, detailed data on emissions as well as fire behaviour and fire spread.

Fire tests on single battery cells and battery packs have been more frequent than large-scale vehicle fire tests. Large-scale vehicle fire tests require additional safety measures and are much more costly compared to cell/module/pack testing. Tests on battery packs and battery modules provide information on risks associated with the battery and support engineering of a fire safe battery design, whilst large-scale fire tests give a holistic view on vehicle fires.

A handful of large-scale fire tests on BEVs have been performed and can be found in for example work by Watanabe et al., [3] Lam et al., [4] Truchot et al., [5] Lecocq et al., [6] and Willstrand et al. [1] These large-scale tests show that a typical passenger vehicle fire lasts for 60 – 90 min and, on average, has a total heat release (THR) of 5.9 ± 1 GJ. [1] The total available chemical energy in a vehicle varies and depends on the vehicle type, size and materials. The peak heat release rate (HRR) for a passenger car fire is typically in the range of 1.5 – 8 MW [2] and also depends on the vehicle size and materials. For example, plastics used for seating/upholstery etc. amount to an average of ~ 20% [7] of the total weight of a passenger vehicle and will considerably affect the combustion behaviour.

All fires release toxic gases, and the quantity and composition depend on the material composition of the combustibles, gas temperature, and the oxygen availability. [8] Gases found in vehicle fire emissions include (but are not limited to) CO, CO_2, NO_x, SO_2, HX, HCN, which all are classed as asphyxiant or irritant gases. PAHs, VOCs, dioxins and a range of metals/metal oxide particles are also found in vehicle fire effluents. [1,2] An overview of substances found in the combustion of ICEVs and BEVs can be found in section 1.2 and in Willstrand et.al. [1]

1.1 Lithium-Ion Batteries

The global battery demand is projected to grow by 25% annually to reach 2 600 GWh in 2030. [9] To satisfy customer needs, the general objective in battery development for electric vehicles is to obtain extended driving ranges and faster charging. As the energy content increases, by increased cell capacity and higher pack voltages, the safety design of battery packs and cells becomes even more important. The current state of the art as well as expected future developments of lithium-ion batteries (LIBs) are summarized in work by for example Tidblad et al. [10] and Armand et al.. [11]

Battery Cell Configuration

A conventional configuration of the materials used for LIBs include a negative electrode (anode), a positive electrode (cathode), an electrolyte, a separator, and current collectors (Figure 1).

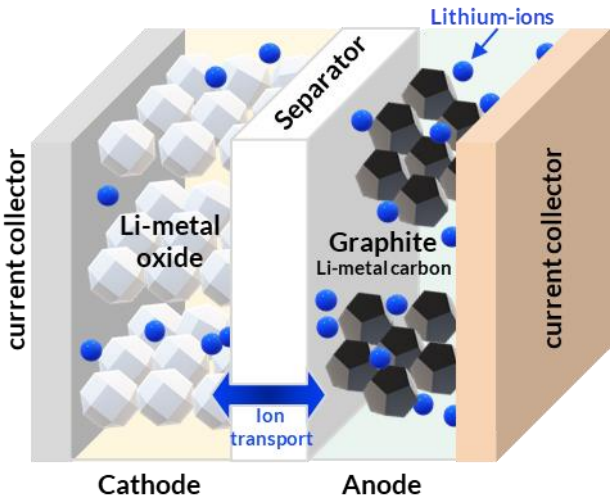

Figure 1. Simplified schematic image of the cell configuration in a lithium-ion battery (sketch is not to scale).

The anode material typically used in commercial applications is graphite. The cathode material comes in a variety of different lithiated materials. For BEVs, $LiFePO_4$ (LFP), $LiNi_xMn_yCo_zO_2$ (NMC) and $LiNi_xCo_yAl_zO_2$ (NCA) are the most frequently used cathode materials. The stoichiometric arrangement, here denoted by x-y-z, of the included metals can also vary. For example, $LiNi_xCo_yMn_zO_2$ comes in a variety of compositions, such as 1-1-1, 5-3-2, 8-1-1 etc. and the composition will influence the performance of the cathode material. To enhance the adhesion of the active material, a binder material is used, for example polyvinylidene fluoride (PVDF).

The electrolyte is composed of an organic carbonate-based solvent (e.g., ethylene carbonate or dimethyl carbonate) that is mixed with a lithium salt, such as $LiPF_6$, $LiClO_4$ or $LiBF_4$.

The separator functions as a physical barrier between the cathode and anode material, providing protection against internal short circuits (ISCs). Separator membranes are commonly made of polymers such as polyethylene (PE), polypropylene (PP) or composites materials of these. Additionally, during charging and discharging the separator functions as an electrolyte reservoir for the transport of lithium ions.

Since battery chemistries are continuously developing, the safety considerations should be assessed for each specific battery chemistry. Safety aspects that are relevant today might change as LIBs develop. As an example, replacing flammable organic liquid electrolytes with solid electrolytes [12,13] may have a pronounced effect on the combustion behaviour of the battery cell.

Thermal Runaway and Fire

Thermal runaway is a form of battery failure which can be caused by mechanical-, electric- or thermal abuse. [14] It can also be initiated by ISC, which can be attributed to chemical crossover [15] but more often to failure of the separator/interphase materials. [16] When separator/interphase materials are damaged, exothermic chemical reactions are initiated between the cathode, anode and electrolyte. The exothermic reactions are followed by an increase in cell temperature and pressure. The increased pressure can eventually lead to cell rupture, which will release a mixture of toxic and flammable gases.

Effect of SOC on Fire Behaviour

The gases released from a thermal runaway will typically self-ignite, which further heats the battery and escalates the thermal runaway propagation. The SOC will affect the HRR from a battery fire, particularly the growth rate and peak HRR. A battery cell with higher SOC generally releases heat faster than a cell with lower SOC. [17–21] However, the SOC has no major influence on the total energy released from combustion of LIBs.

Effect of Cathode Material on Fire Behaviour

In work by Wang et al., [22] the thermal reactivity of cathode material categories was ranked LCO>NCA>NCM>LMO>LFP. However, the variation within these categories is large, for example among different NCM materials, which affects the ranking order. The reactivity is determined by the chemical reactions of the cathode material, i.e. the oxygen release and the heat release of the reaction. The onset of these reactions range between 130 – 300°C. [22]

Effect of Electrolyte on Fire Behaviour

Conventional electrolytes used in LIBs have low flash points and burn readily. The electrolyte can thermally decompose when the temperature exceeds ~ 200°C and reacts with the lithium salt. Some of the compounds found when electrolyte and lithium salts are exposed to high temperature are water vapor (H_2O), hydrogen (H_2), carbon dioxide (CO_2), carbon monoxide (CO), methane (CH_4), fluorinated gases (such as HF, POF_3) and fluorinated alkanes. [23–25] However, chemical reactions that lead to pressure build-up inside the cell can already be found at cell temperatures below 100°C (organic and inorganic solid electrolyte interphase (SEI) decomposition). [26]

In a study by Ribière et.al., the effective heat of combustion for a LIB cell was determined to ~ 4.0 MJ kg^{-1}, where the electrolyte contributed to almost half of that (1.92 MJ kg^{-1}). [19] Therefore, the electrolyte represents a significant source of energy upon ignition of the battery cell, even if the mass fraction is low (~ 10% of the cell mass). [27] The electrolyte together with the separator material account for approximately 80% of the heat released from a LIB fire. [19,27]

1.2 Substances Found in Vehicle Fires

The following sections will briefly address some frequently encountered substances found from vehicle fires. A more extensive compilation of combustion products can be found in work by for example Lönnermark and Blomqvist, [2] and Willstrand et al.. [1] Fluorinated compounds will be covered in more detail in section 1.3.

Particulate Emissions

Particulate emissions consist of incomplete combustion products. Additionally, dioxins, PAHs and metals tend to bind to these particulates. Research on the health effect of particulates in air indicate that exposure to particulate matter (PM) in ambient air can cause cardiovascular and respiratory health effects. Particles with an aerodynamic diameter less than 10 μm (PM_{10}) are considered as suspended pollutants and have an

adverse effect on the respiratory system. The annual average of PM_{10} concentrations in ambient air in Europe is about 15 to 60 μg m^{-3}. [28]

Polycyclic Aromatic Hydrocarbons

PAHs are a class of organic compounds found upon combustion. The amount and type of PAHs formed depend on several factors, for example on the availability of oxygen, moisture content and surrounding temperature. This study focuses on the 16 PAHs listed by the US Environmental Protection Agency (EPA) as priority air pollutants. PAHs come in different molecular weights (sizes) and have different oxidative potentials in human metabolism. This renders them harmful to humans as well as to the environment. [29] A high PAH molecular weight correlates with a high oxidative potential, which may lead to severe DNA damage. PAH with a high molecular weight therefore pose a greater health risk to humans. [30]

Volatile Organic Hydrocarbons

VOCs are formed upon incomplete combustion of organic materials. Benzene, toluene, and styrene are amongst the most frequently found VOCs. Many VOCs are found to be either cancerogenic, allergenic, affect the central nervous system and some can even be acutely toxic. Additionally, VOCs can increase the formation of ground-level ozone which may result in premature aging of plants and crops. [31,32]

Inorganic Compounds

A range of different inorganic species can be found in the combustion products of vehicles. Concerning health and environment, heavy metals (such as arsenic, lead, cadmium etc.) are considered as the more severe pollutants due to their persistency and possible adverse effects on health. In a review by Briffa et al., [33] the pharmacokinetics and toxicological processes in humans for a variety of heavy metals and how these pollutants enter the environment are described in more detail.

1.3 Fluorinated Compounds Found in LIBs

In 2022, Rensmo [34] conducted a literature review to establish various fluorochemicals found in LIBs. Fluorochemicals could be found in the binder material, electrolyte salts, electrolyte additives and fluorinated derivatives of the electrolyte.

In work by Hu et al., [35] complex gas formation was investigated after mechanical and thermal treatments of LIB cells. A total of 46 gaseous species were characterised. Fluorochemicals such as CHF, CH_3F, CF_4, COF_2 and SiF were detected. A list of the fluorinated compounds found in LIBs and their origin can be found in Appendix 1.

Many of these fluorinated compounds are used to improve the performance and lifetime of LIBs. Therefore, substitution of these compounds, without having deteriorating performances of the LIB, may be difficult. Note that fluorinated compounds are also found for example in tubing and hoses (PVDF and PTFE), electronics, anti-static coatings, as well as in the air conditioning refrigerants.

Hydrogen Fluoride in BEV Fires

An increased concentration of gaseous hydrogen fluoride (HF) has been reported for BEV fires in comparison to internal combustion engine vehicle (ICEV) fires [1], see Figure 2. HF is known to be very hazardous; highly concentrated (> 20 wt.%) solutions of HF can even have life-threatening effects. [36]

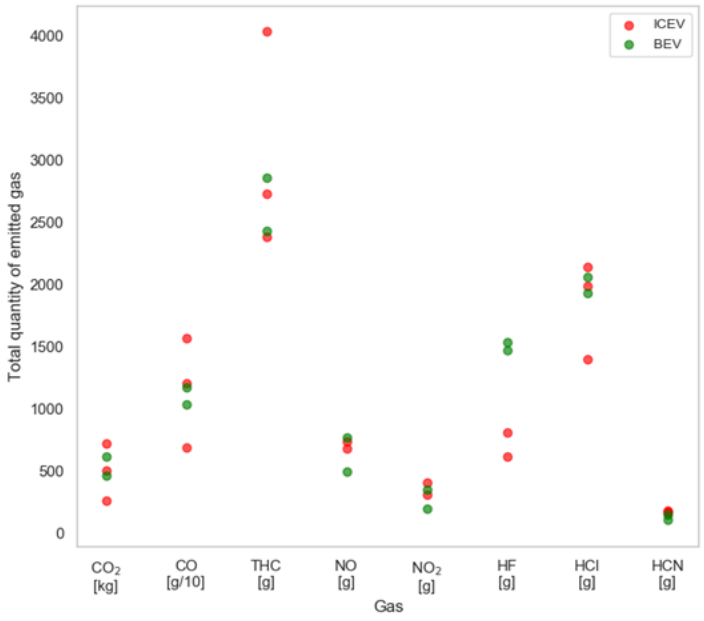

Figure 2. Total quantity of emitted gas from large-scale tests on passenger cars. The graph is re-printed with permission from reference [1]. Red and green dots represent quantities for ICEV and BEV, respectively. The y-axis scale is found below each gas analysed (on the x-axis).

The potential dangers of HF have caused a huge interest and concern by the public, as well as from fire and rescue services. Since the early reports on HF from LIB fires, plentiful of studies have been performed to thoroughly investigate the possible dangers of HF released during combustion of lithium-ion batteries.

For example, Wingfors et al. [37] studied the HF penetration of standard fire suites, as well as the risk of dermal uptake of gaseous HF. The dermal uptake of gaseous HF ranged between 7 to 118 mg per 18 000 cm² of skin area (18 000 cm² is the average skin area of an adult human) and the protection factor of the fire suits used varied between 10 and 260 with an average of 120. This means that the concentration of HF, on average, was 120 times lower on the inside of the fire suit than on the outside. The study concluded that adverse health effects caused by skin exposure to HF during firefighting is very unlikely. Additionally, Dennerlein et al. studied the dermal penetration of HF in solution. It was found that upon a 24 h exposure to HF, in concentrations varied between 5 – 30 wt.%, only a small amount (~ 1%) was able to penetrate the skin. Increasing the HF concentration to 50 wt.% led to a skin penetration of 8%. [38] Note that the HF released from combustion of lithium-ion battery cells is commonly analysed in the gaseous form and in much lower concentrations.

Furthermore, using data from Dennerlein et al. [38] and Wingfors et al. [37] the ambulance service in Stockholm (AISAB) published a video on YouTube (21 Dec 2021) where they estimated different lethal doses of HF depending on the type of HF

exposure (dermal uptake or inhalation). For a highly concentrated solution of HF (50 wt.%), an exposure of 1% of the body area (roughly the size of your palm) would be required for a deadly dose (5 – 30 mg kg^{-1}), whilst an HF solution of 5 wt.% would require an exposure of 160% of the body area. [39] A deadly dose through inhalation, would require an exposure to 100 ppm of HF for about 2 – 12 h (considered heavy breathing of 2 400 L h^{-1}). [39] Such high concentrations for such prolonged times would in practise be unbearable to withstand. In the gaseous form, a concentration of HF > 30 ppm is namely irritating for eyes and nose, and the highest concentration tolerable for more than 1 min is around 122 ppm. [40]

The reported concentrations of HF detected upon combustion of BEVs/ICEVs/batteries vary to a large extent. Larsson et al. estimated that 20 to 200 mg W^{-1} h^{-1} of HF could be released from an EV fire. [41] In previous work, a comparison between different battery fire tests and HF emissions were made, where the HF emissions ranged between 20 to 5 000 ppm calculated for a reference volume of 1 000 m^3. [1] This indicates that there is a large discrepancy for the reported HF concentrations.

In a study by Lombardo et al. [42] incineration of LIBs was studied. HF and other organic fluoride containing by-products were found as a result from the degradation of the binder material, PVDF. It is therefore important to consider that the analysed fluoride ions, in e.g., extinguishing water, may have a different origin than HF, such as other organic by-products containing fluoride.

1.4 Environmental Consequences of Vehicle Fires

Fires contribute to contamination of air and, depending on the tactic used by the fire and rescue services, possibly also to surface waters, groundwater and soil. Additionally, the environmental impact of the fire will depend on the size of the fire and suppression media used. [43]

In 2016, Kärrman et al. [44] studied the environmental impact from different firefighting tactics and use of different suppression media, such as foams and additives. All tested foams and additives were toxic against water living organisms. The most environmental benign firefighting tactic was to not extinguish the fire at all. However, for some fires this option is not feasible. Instead, a quick response and little usage of water would yield the most environmental benign firefighting operation. Furthermore, fires in vehicles imply a smaller threat to the environment compared to larger fires in for example chemical storage facilities or warehouses. [45]

Extinguishing Water

Extinguishing water from fires contain a variety of toxic combustion products. The concentration and type of compounds will depend on many factors, such as the material combusted, the fire scenario, suppressant used, and the volume of water/suppressant used. In a study by Lönnermark and Blomqvist, [2] it was found that extinguishing water from ICEV fires were severely contaminated and contained a high concentration of suspended substances and a high organic content. Amongst the metals found in the water, lead, copper, zinc, and antimony were reported as the more severe contaminants.

Risk Assessment of Contaminated Sites

The Swedish Environmental Protection Agency (Naturvårdsverket) has published a report on the risk assessment of contaminated sites, report 4918, [46] which is summarised in the following sections. An English review on environmental risk assessment resulting from fires can be found in for example Martin et al.. [47]

To identify risks and hazards of fire effluents at a particular site, evaluation of the chemical toxicity and concentration, long-term effects, sensitivity of recipients and rate of dispersion of pollutants is required.

Risk Classification of Contaminants

Initially, an analysis of the existing contaminants needs to be performed. Data can be collected from different sources, for example from air, soil, groundwater, surface water and/or sediment. The severity of pollution of the area can then be judged by analysis of the samples. According to reference [46], if the concentration of contaminant is >3 times higher than the guideline value, the condition of the polluted area can be judged as “very serious”.

Table 1 is obtained from reference [46] and presents the inherent risk of different compounds. The overall risk of a certain compound is a combination of the inherent risk and the concentration/volume present. Surface water guideline values for a selection of compounds are presented in Table 2.

Table 1. Inherent risk-classification of compounds, taken from reference [46]

Low to Moderate	**High**	**Very high**
Iron	Cobalt	Arsenic
Calcium	Cupper	Lead
Magnesium	Chromium (III)	Cadmium
Manganese	Nickel	Chromium (VI)
Paper	Vanadium	Sodium (metal)
Wood	Ammonium	Benzene
Aluminium	Aromatic hydrocarbons	Cyanide
Metal scrap	Phenol	PAH
Acetone	Formaldehyde	Chlorinated solvents
Aliphatic hydrocarbons	Glycol	Dioxins
Wood fiber	Acid and bases	PCB
Bark	Organic solvents	Chlorinated aromatics
Zink	Hydrogen peroxide	Pesticides
	Paints	
	Petroleum products	
	Fuels	
	Wood tar	

Table 2. Surface water guideline values for some of the inorganics analysed in this work

Analyte	Abbreviation	Guideline value (µg L^{-1})	Reference
Aluminum	Al	1 – 4800 170	[48] [49]
Boron	B	1500 – 29000	[50]
Chromium	Cr	15 – 150	[46]
Cobalt	Co	4 – 100	[51]
Copper	Cu	9 – 90	[46]
Lithium	Li	2500	[52]
Nickel	Ni	45 – 450	[46]
Manganese	Mn	430 – 3600	[53]
Molybdenum	Mo	73	[54]
Lead	Pb	3 – 30	[46]
Antimony	Sb	10 – 100	[46]
Zinc	Zn	60 – 600	[46]
Chloride	Cl^-	120000 – 640 000	[55]
Fluoride	F^-	120 – 500	[56]
Bromide	Br^-	-	n.a

Note that the guideline values for metals/ions may be affected by water hardness and pH which should be considered upon evaluation. Additionally, for guideline values from reference [46], the lower number indicate a lower biological risk, whereas the higher number indicate a high risk.

Surface Water Guideline Value of Lithium

There is no surface water guideline value for lithium in Sweden. According to a study carried out by Schrauzer, [57] surface waters contain between 1 – 10 µg L^{-1} lithium. The concentration of lithium in drinking water from Swedish wells range between 0.03 – 177 µg L^{-1} (median 6.7 µg L^{-1}). [58]

Lithium concentrations above 1 mg L^{-1} in drinking water have been associated with impaired thyroid and calcium homeostasis during pregnancy. [58] The aquatic toxicity of lithium varies depending on the organism studied. For *Daphnia magna* (crustacean) the effective concentration (EC_{50}) was found to be 33 – 197 mg L^{-1} whilst the reported EC_{50} for *Pimpehales promelas* (fish) was much lower, between 1 – 6.4 mg L^{-1}. [59]

Fluoride Toxicity to Aquatic Organisms

The fluoride concentration for unpolluted fresh waters generally ranges from 0.01 – 0.3 mg L^{-1}, and between 1.2 – 1.5 mg L^{-1} for unpolluted seawaters. [60] Fluoride can have severe effects on aquatic species living in soft waters. For hard waters or sea waters, the

fluoride toxicity is less severe because the bioavailability of fluoride ions is reduced with increasing water hardness.

Fluoride lethal concentration (LC_{50}) varies with aquatic organisms, exposure time and even with water temperature for higher living organisms. [60] For algae, the fluoride concentration in both sea water and fresh water can have growth inhibitory as well as growth enhancing effects. The growth inhibitory or enhancing effect depends on the fluoride concentration, exposure time and algae species. [60]

The fluoride toxicity to aquatic invertebrates increases with increasing fluoride concentration, increased exposure time and will vary with water temperature. For *Daphnia magna* (crustacean), LC_{50} values of fluoride ions vary between 205 [61] – 352 [62] mg L^{-1} at 24 h of exposure.

In a study by J.A. Camargo et.al., [60] it was suggested that the levels of fluoride ions should be kept below 500 μg L^{-1} to protect the caddisfly larvae (and higher-organisms that prey on them) from fluoride pollution. The Canadian *Water Quality Guidelines for the Protection of Aquatic Life* specify a guideline value of 120 μg L^{-1} of fluoride in fresh waters. [56]

Distribution of Pollutants and Sensitivity of Recipients

When the inherent risk and concentration/volume of the pollutants have been determined, the next step in the risk analysis is to determine how fast these contaminants may spread from the accident site. To determine the exact rate of propagation of pollutants would require tremendous efforts. Therefore, the following points should be considered:

- Geology and hydrology of the site.
- Chemical properties of the soil/ground.
- Pollutant localisation at testing.
- Surrounding buildings, facilities and technical installations.
- Compatibility of the pollutant and the surrounding environment.

The distribution of pollutants down to the ground water is affected by arrange of factors such as the type of pollutant, the flow rate, ground/soil type, buildings, technical installations etc. The Geological Survey of Sweden (SGU) has published an open access “Geomap” [63] application that can be used to assess the geology of the site. The distribution of pollutants is thereafter weighed with the sensitivity of recipients and the specific protection value of the site.

A range of factors will affect the severeness of pollution. Therefore, it is important to remember that each polluting scenario needs to be assessed individually. Additionally, effects of dilution need to be considered.

2 Methods

2.1 Fire Tests

Three large-scale vehicle fire tests and one battery fire test were performed in the large fire hall at RISE, Borås. The fire hall is equipped with a calorimeter hood to enable collection and analysis of smoke and gas emissions. An overview of the test setup can be found in Figure 3. Advanced flue gas reduction and water purification systems are used to minimise exhausts to the environment upon testing in the fire hall.

Extinguishing water was collected through a tray-pump system (see Figure 4), where the extinguishing water was pumped to an adjacent hall for sampling. This setup was chosen for safety reasons, as no personnel were allowed in the fire hall during testing.

The tested vehicles comprised of one BEV where the battery pack had been removed (reference test), one complete BEV and one ICEV of the same model as the BEV. Additionally, a separate battery fire test was performed using the battery pack that had been removed from the BEV mentioned above. Specifications of the test objects are presented in Table 3. All vehicles as well as the battery were brand new and came from the same manufacturer, which enables a good comparison.

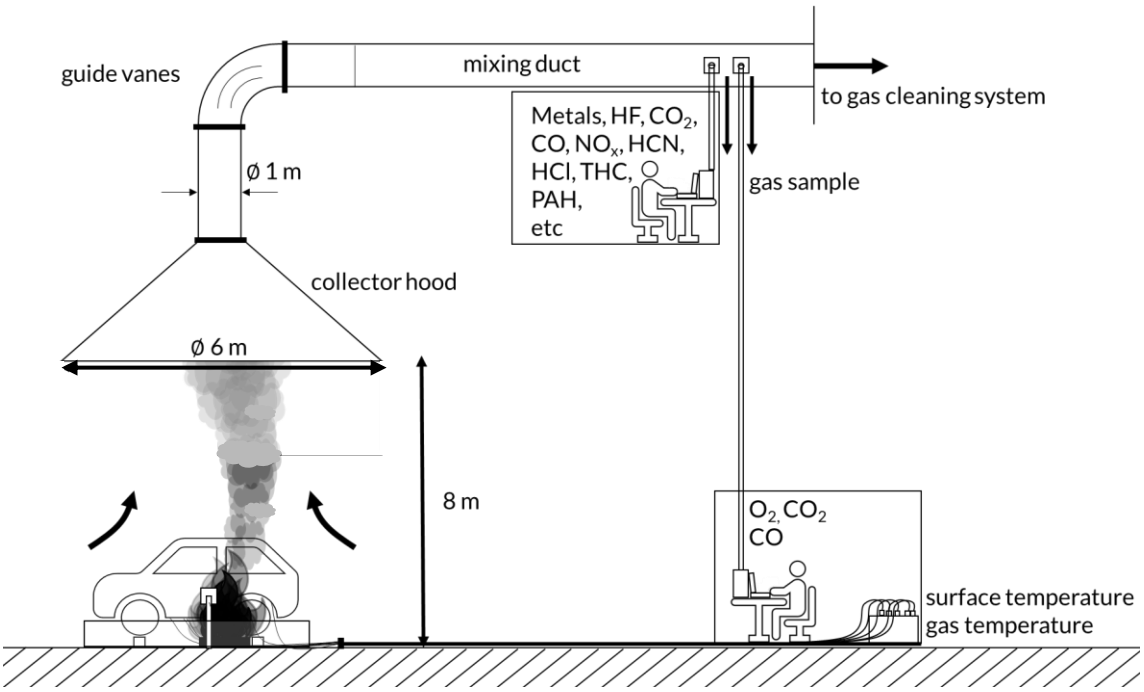

Figure 3. Schematic of the large fire hall, test setup and measurement setup. Adapted figure from reference [1].

2.1.1 Test Objects

The test object specifications are listed in Table 3. Certified automotive technicians checked the status of the battery packs, and no fault-codes were detected prior to the tests. For safety reasons, some modifications of the vehicles were necessary. The modifications included to puncture the tyres and to disable dampers and suspensions. No active airbags were present in the tested vehicles. For convenience considering the

burner placement, the plastic shield covering the underneath of the vehicle was removed for all tested vehicles.

Table 3. Specifications of the tested vehicles, all from the same manufacturer and of same model

Test	Type	Traction energy	SOC (%)	Cell type	Model	Year
1	BEV	Battery removed	-	-	Small SUV	2021
2	ICEV	Petrol, 40 L	-	-	Small SUV	2021
3	BEV	50 kWh	90	NMC	Small SUV	2021
4	Battery	50 kWh	90	NMC	216 cells	2021

2.1.2 Test Setup

A propane gas burner (dimensions: 0.4 × 0.1 × 0.1 m) with a nominal output of 30 kW was used for ignition and was kept at that level throughout the test. The burner was kept active as a safety measure to enable ignition of battery vent gases in case the sprinklers would extinguish the fire (flames).

Test 1 (Table 3) was used as a reference test for test 2 and test 3; test 1 was a free burning test and the vehicle did not carry an energy storage. In the reference test and in the ICEV test, the vehicles were ignited with the burner placed below the engine compartment of the vehicle. For the BEV and the battery pack, the burner was located below the rear of the battery pack to ensure involvement of the battery in the fire as early as possible. The stand-alone battery pack was shielded above it to reduce direct water exposure from the sprinkler system to the battery casing (representing the protection of the chassis).

For safety reasons the amount of petrol in the tank was kept at 20 L. The remaining petrol (20 L) was poured into a tray (1.0 × 1.1 × 0.1 m) below the tank to mimic a leaking tank and resulting pool fire.

Smoke and gases generated during tests were exhausted through the collector hood to the gas cleaning system. The distance between the hood and the ground was ~ 8 m. The flow rate in the duct in all three tests was ~ 25 $m^3 s^{-1}$.

For all tests, a large steel tray (5.0 × 2.0 × 0.15 m), equipped with a water outlet connected to a pump, was positioned under the vehicle/battery to collect water from the sprinklers (see Figure 4).

2.1.3 Sprinkler System

To enable analysis of extinguishing water from the sprinkler water, a system that could deliver water homogeneously for all tests and that could be operated remotely was required. A sprinkler system was considered as the best alternative.

The sprinkler heads used in the tests were upright TYCO model Series TY FRB, Quick Response, Standard Coverage. Normally, these sprinkler heads are fitted with a 3 mm glass bulb with a nominal operating temperature of 68°C. However, prior to the tests the glass bulbs were removed to enable remote operation of the system. The sprinkler heads have a nominal K-factor of 80.6 $\frac{L\,min^{-1}}{\sqrt{bar}}$ and were operated to give a water discharge density of 10 mm min^{-1}, corresponding to 93 L min^{-1} per sprinkler and a total

flow rate of 372 L min^{-1} since four sprinkler heads were used. The sprinkler system was active for 30 min in each test, resulting in a total water usage of in 11 160 L per test. For reference, the Fire Protection Research Foundation (NFPA) in USA performed several large-scale sprinklered fire tests with BEVs and reported that, upon suppression, between 1 000 and 10 000 L of water was used to extinguish the fires. [64]

The four sprinkler heads were installed in a hydraulically balanced pipe-work, having a sprinkler spacing of 3.05 m by 3.05 m (10 ft. by 10 ft.). Each of the sprinkler heads thus covered an area of 9.3 m^2. The vertical distance from the deflector of the individual sprinkler heads and the bottom of the tray was 2.85 m. A plate thermometer was placed in the centre of the pipework and a pressure transducer was installed at the end of one of the branch lines. The vehicle/battery pack was positioned with its centre point (the centre point between the four tires) at the centre of the four sprinklers.

The distribution line of the pipework had a solenoid valve that was remotely operated when the fire size reached a convective heat release rate of 667 kW (estimated convective HRR for an operating temperature of 68°C for the sprinklers), corresponding to a total heat release rate of ~ 1 MW. For the battery fire test, the activation time was set to 30 s after venting. The sprinkler system was scheduled to be active for 30 min during each test. However, in the BEV test, activation was performed in two steps, see further results section.

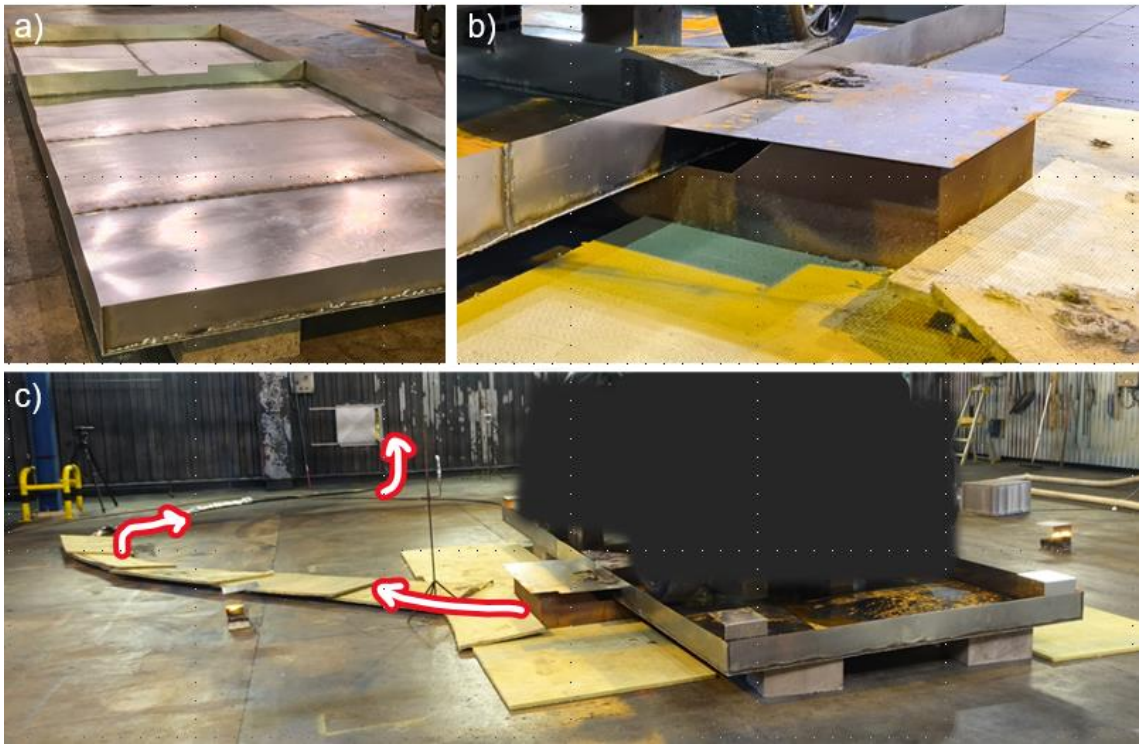

Figure 4. Water collection system, showing a) the large tray, 5 x 2 m, b) small pump tray and c) the complete setup, where red arrows indicate the route of the pumped water to the adjacent test hall.

2.2 Analysis methods

2.2.1 Heat Release Rate

To calculate the HRR, an industry calorimeter was used. The calorimeter collects combustion products through the hood and extracts them through a large exhaust duct. A set of guide plates and a sufficient length of the duct (~ 30 m) have been used to decreases the air turbulence in the exhaust duct. Equations used for the calculation of HRR can be found in reference [1].

Since the experiments included activation of a sprinkler system, a higher humidity as well as some losses related to the collection of gas can be expected. Therefore, the HRR values reported for the tests having the sprinkler system active can be expected to include a larger measurement uncertainty compared the free burning test (test 1 - reference test). A certain overestimation of the HRR can be expected due to the increased air humidity upon the activation of sprinklers. No measurement of air humidity was performed during the tests. An underestimation of the HRR can however also be assumed as there were evident losses (visual) in the total amount of gas collected by the hood.

2.2.2 Temperature

Type-K thermocouples were positioned at different locations (illustrated in Appendix 2, Figure A1) on each vehicle and battery, to monitor how the temperature developed during the test. Additionally, a pair of plate-thermometers were placed at the centre of each long side of the vehicle at a distance of 1 m, and one plate-thermometer was placed 8 m behind the vehicle/battery, to examine the radiated heat during the tests.

2.2.3 Gas Analysis

Gas analysers were installed in close vicinity to the exhaust duct to measure the composition of combustion products, as seen in Figure 3. An overview of the equipment used, and their purposes are presented in Table 4.

Table 4. Targeted analytes in the combustion gases and measurement techniques used

Measurement technique	Analyte	Abbreviation
FTIR spectroscopy	Hydrogen Fluoride	HF
	Hydrogen Chloride	HCl
	Hydrogen Bromide	HBr
	Carbon Dioxide	CO_2
	Carbon Monoxide	CO
	Hydrogen Cyanide	HCN
	Sulphur Dioxide	SO_2
	Nitrogen Dioxide	NO_2
	Nitric Oxide	NO
FID	Total Hydrocarbons	THC
Gas washing bottles	Fluoride ions	F^-
	Chloride ions	Cl^-
	Bromide ions	Br^-

For gas analysis, a ThermoFisher Antaris Fourier Transform Infrared (FTIR) instrument with a 0.2 L heated gas cell and a spectral resolution of 0.5 cm^{-1} was used. Sampling was performed using a heated ceramic particle filter (FTIR pre-filter) and a 10 m heated PTFE sampling line with a sampling flow rate of 3.5 L min^{-1}. The sampling equipment and cell were heated to 180°C. The ceramic filter was dispatched to an external laboratory for analysis of fluoride, chloride and bromide using high pressure ion chromatography (HPIC).

A SICK MAIHAK Model 3006 THC-analyser with a Flame Ionization Detector (FID) was used to detect total hydrocarbons released during tests. The analyser was calibrated against a known concentration of propane (9 000 ppm). Sampling was done similarly to that of the FTIR sampling, through a separate heated ceramic filter and a heated PTFE sampling line, both heated to 180°C. Gases were extracted at a sampling flow rate of 1.0 L min^{-1}.

Additionally, non-filtered fire effluent was collected and sampled using gas-washing bottles. Gas-washing bottles containing a carbonate buffer were used to sample water-soluble halogens. These solutions were analysed by an external laboratory using HPIC.

2.2.4 Soot Analysis

Sampling of soot content in the exhaust duct was performed through isokinetic sampling to quartz filters. Sampling was made using a flow rate of 50 L min^{-1} and the sampled gas flow was divided between two identical filters. One of the filters was analysed for metals and water-soluble anions of fluoride, chloride and bromide (F^-, Cl^- and Br^-), the other filter was analysed for 16 types of PAHs.

Filters were dried in ambient temperature before analysis. Substances analysed are presented in Table 5. The filter was dissolved in nitric acid (240°C), and extracts were analysed for inorganic species using inductively coupled plasma mass spectroscopy (ICP-MS) and optical emission spectrometry (ICP-OES). For analysis of PAHs, the filter was extracted with toluene in an ultrasonic bath for 30 min. Naphthalene-d, chrysene-d and benzo[a]pyrene-d were used as internal standards.

Table 5. Targeted particulate bound analytes and measurement techniques used

Measurement technique	Analyte	Chemical formula	Type
Isokinetic gas sampling on filters	Soot	-	Solid
ICP-MS and ICP-OES	Aluminium	Al	Metal
	Boron	B	Metal
	Mercury	Hg	Metal
	Lead	Pb	Metal
	Cadmium	Cd	Metal
	Cobalt	Co	Metal
	Nickel	Ni	Metal
	Chromium	Cr	Metal
	Copper	Cu	Metal
	Tin	Sn	Metal
	Vanadium	V	Metal
	Zink	Zn	Metal
	Antimony	Sb	Metal
	Arsenic	As	Metal
	Lithium	Li	Metal

Measurement technique	Analyte	Chemical formula	Type
	Molybdenum	Mo	Metal
	Manganese	Mn	Metal
IC-analysis	Fluoride	F-	Anion
	Chloride	Cl-	Anion
	Bromide	Br-	Anion
GC-MS analysis	16-PAHs	-	Organic

2.2.5 Extinguishing Water Sampling and Analysis

To reduce uptake of existing contaminants from the fire hall and to enable collection of the extinguishing water, a customised steel tray (5.0 x 2.0 x 0.15 m) was placed beneath the test object. The collected water in the tray was led by two openings to a smaller pump tray (0.15 m^3). The pump tray was located lower than the large tray, and from there the collected water was pumped to an adjacent test hall for sampling into clean flasks for further analysis. Photos of the sampling setup are shown in Figure 4. The pump delivered ~ 3 600 L of water in 30 min, i.e., roughly a third of the total water delivered by the sprinkler system was collected during each test. The remaining water was collected and cleaned using the water purification system connected to the fire hall.

The large tray beneath the vehicle was exchanged to a new tray between test 2 (ICEV) and test 3 (BEV). The pump tray and the connected hose were not exchanged between the tests. Therefore, background water sampling (blank sample) was performed before each test to evaluate any remaining contamination from previous tests or from the fire hall itself. Blank samples were taken by flushing the whole test setup with clean tap water for a minimum of 10 min before each test. The water used for flushing (at t = 10 min) was taken as the blank sample.

The collection of extinguishing water for all tests started when the sprinkler system was started. A heavy-duty pump was used to pump the water from the pump tray at a flow rate of ~ 2 L s^{-1}. One litre of water was collected for sampling each minute for the time that the sprinkler system was active. At the end of the test, 0.5 L of the water left in the large tray was also taken for analysis.

In total, five samples from each test were formed: (1) 0-10 min, (2) 10-20 min, (3) 20-30 min, (4) 0-30 min (equal mixture of samples 1 - 3) and (5) sample taken from the tray at the end of the test. Analysis performed on the water samples were the same as the ones presented for soot in Table 5. Additionally, VOCs as well as per and polyfluoroalkyl substances (PFAS) were analysed using gas chromatography-mass spectrometry (GC-MS) and liquid chromatography-mass spectrometry (LC/MS/MS), respectively.

For analysis of the inorganic species, water samples were filtered (0.45 µm) before determined by Inductively Couples Plasma Mass Spectroscopy (ICP-MS) and ICP Optical Emission Spectrometry (ICP-OES). Water-soluble contents of fluoride, chloride and bromide was analysed using ion chromatography (IC) with a conductivity detector.

For analysis of VOC, water samples (100 ml) were extracted with dichloromethane (DCM) after addition of internal standard bis(2-ethylhexyl) phthalate (DEHP-d). The extracts were evaporated to 0.2 to 0.5 ml followed by GC-MS. Detected compounds were identified using NIST library of mass spectra and the concentrations were

determined in equivalents of internal standard DEHP-d. Another part of the samples (10 ml) was analysed by headspace GC-MS after heating at 95 °C for 30 min. The compounds detected were identified by NIST library of mass spectra and the concentrations were determined in equivalents of internal standard benzene-d. The PAH concentration in the water samples was analysed by GC-MS, using 16 external standards (listed in Appendix 6) after extraction with DCM.

PFAS were analysed using liquid chromatography tandem mass spectrometry (LC/MS/MS). The LC/MS/MS instrument was a Waters Acquity UPLC I-class LC-system and a Waters Xevo TQ-XS mass spectrometer. A Waters Acquity UPLC BEH C18, 2.1 mm × 100 mm, 1.7 µm column was used for chromatographic separation of the analytes. Sample preparation and analysis was made according to ASTM D7979-19 "Standard Test Method for Determination of Per- and Polyfluoroalkyl Substances in Water, Sludge, Influent, Effluent, and wastewater by Liquid Chromatography Tandem Mass Spectrometry (LC/MS/MS)".

2.2.6 Biological Characterisation of Extinguishing Water

Biological characterisation was performed by an external laboratory, Toxicon AB. Samples taken from the large tray at the end of each test (ICEV, BEV and battery test) were frozen and sent to Toxicon for analysis. pH, salinity and conductivity were measured before characterisation, and were buffered if needed.

Microtox

Microtox analysis was performed on all samples according to SS-EN ISO 11348-3:2008 (mod.) "Determination of the inhibitory effect of water samples on the light emission of *Vibrio fischeri* (Luminescent bacteria test)". Salt content and pH were adjusted to 20 ‰ and 6.8 – 7.2, respectively, before testing.

Green Algae

Growth inhibition rate (E_rC_{10} and E_rC_{50}) of *Pseudokirchneriella subcapitata* (Green algae) was evaluated on water samples from the ICEV and BEV test according to SS-EN ISO 8692:2012 "Fresh water algal growth inhibition test with unicellular green algae". pH was adjusted to 8.1 ± 0.2 before testing.

Daphnia Magna

Half maximal effective concentration (EC_{50}) for *Daphnia Magna* (Crustacean) was determined for samples from the ICEV and BEV using SS-EN ISO 6341:2012. "Determination of the inhibition of the mobility of *Daphnia magna Straus* (Cladocera, Crustacea) - Acute toxicity test". The pH from the ICEV fire test sample had to be adjusted before the analysis.

3 Results and Discussion

Temperature graphs for all tests are found in Appendix 2, while results from gas and soot analyses are found in Appendix 3 and 4. The extinguishing water analysis results are found in Appendix 5 and 6.

For all tests conducted, ignition of the burner was performed at t = 5 min. Sprinkler system activation, peak HRR and visual observations for each test are summarised in Table 6.

Table 6. Time of ignition, peak HRR, sprinkler activation, visual observations regarding energy storage and thermal runaway (TR) and weight before/after test of vehicles/battery

Reference		**ICEV**		**BEV**		**Battery**	
Weight before test							
1 170 kg		1 200 kg		1 540 kg		340 kg	
Time (mm:ss) and observation							
05:00	Ignition	05:00	Ignition	05:00	Ignition	05:00	Ignition
15:00	First peak HRR	06:21	Pool fire ignited	09:00-10:00	First signs of TR[1]	37:55	Puff of white smoke
45:00	Second HRR peak	07:58	Sprinklers activated*	09:50	Sprinklers activated*[3]	60:00	Increase of burner to 70 kW
90:00	Test terminated	10:53	Fuel tank rupture	10:00	First peak HRR	60:00	TR[1,2]
		10:55	First peak HRR	31:20	Second peak HRR	60:30	Decrease burner 30 kW
		37:58	Sprinklers deactivated	34:50	Sprinklers activated	60:30	Sprinklers activated[4]
		52:36	Second peak HRR	36:30	TR[2]	62:36	Peak HRR
		100:00	Test terminated	56:30	Sprinklers deactivated	100:00	Test terminated
				106:48	Third peak HRR		
				150:00	Test terminated		
Weight after test (percentage mass loss)							
930 kg (20.5%)		892 kg (25.7%)		1 213 kg (21.2%)		266 kg (21.8%)	
*HRR = 1 MW, [1]Gas temperature above 600°C (battery), [2]Visible signs of thermal runaway (TR), [3]active for 10 min, [4]30 s after visible TR active for 30 min							

3.1 Heat Release Rate

The HRR, both total and convective, were calculated for all four tests (Figure 5, a-d). The reference test was a free burning test, whilst the sprinkler system was activated in the remaining three tests (duration marked blue in Figure 5).

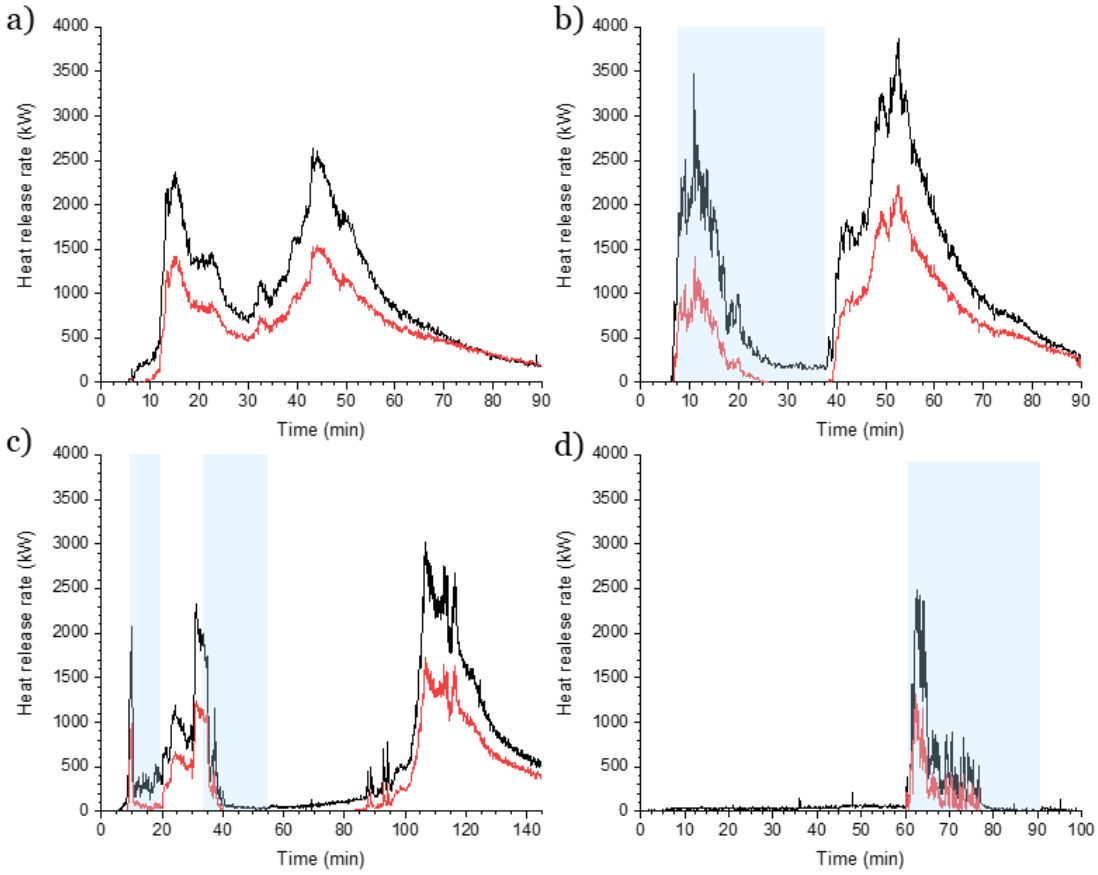

Figure 5. Total (black) and convective (red) heat release rate for (a) reference test, (b) ICEV, (c) BEV and (d) battery test. Blue shading indicates when the sprinkler system was active. The total heat released were a) 5.0 GJ, b) 6.1 GJ, c) 5.7 GJ and d) 0.8 GJ

3.1.1 HRR Reference Test

For the reference test (vehicle without energy storage), the HRR graph displays two peaks. This is contradictory to fire tests in previous work [1], were only one HRR peak was found for all tested vehicles. The reason for the "split peak" in the reference test can be explained by the fire propagation. The tested vehicle was ignited using a burner placed at the front of the vehicle (beneath the engine compartment) and since the vehicle did not carry any energy storage, the first peak is solely from the engine compartment as well as plastic details in the front of the car that are burning. The passenger cabin was intact until test time ~ 30 min, which until then slowed down fire propagation towards the back of the vehicle. Furthermore, removal of the plastic protection underneath the vehicle may also have inhibited fire spread at the bottom of the vehicle.

At 30 min (25 min after ignition of the burner) the left front window collapsed, resulting in ignition of the interior of the passenger cabin. Consecutively, involvement of the rear (rear tyres, bumper etc.) of the vehicle in the fire resulted in a second HRR peak (Figure 5a).

The total heat release (THR) for the vehicle without energy storage was 5.0 GJ. The first part (t = 0 – 30 min) constituted of 28% of the total heat release (THR) whereas the second part (30 – 90 min) amounted to 72% of the THR.

3.1.2 HRR ICEV Test

For the ICEV test, the pressure in the test hall fluctuated during the activation of the sprinkler system, resulting in a smoke-filled hall during the time that the sprinklers were active. The consequence of this was that less smoke and gas were extracted to the calorimeter hood and the losses likely imply an error giving too low measurement values (i.e., the amount/concentration were likely higher than reported).

For the ICEV, the sprinkler system was kept activated for a pre-set time of 30 min. The HRR graph is presented in Figure 5b. The HRR continued to increase after activation of the sprinkler system and reached its maximum 2 min and 57 s after activation. The first peak HRR can be assigned to the burning petrol pool and the subsequent rupture of the fuel tank. When the petrol had been combusted, the HRR steadily declined, reaching a "steady state" value of ~ 175 kW during the last 10 min when the sprinkler system was activated.

The sprinkler system was turned off at test time 37:58. At 45:00 the back windows ruptured and the passenger cabin was involved in the fire, leading to a second HRR peak. The THR for the ICEV was 6.1 GJ. The first peak (0 – 35 min, sprinklers active) constituted of 26% of the THR whereas the second peak (35 – 90 min) amounted to 74% of the THR.

3.1.3 HRR BEV Test

In the BEV test the burner was placed beneath the rear part of the battery pack (rear end of vehicle), in contrast to the reference test and the ICEV test, to activate the battery as early as possible in the test.

Activation of the sprinkler system was initiated when the HRR reached 1 MW, as in the ICEV test. However, upon activation of the sprinkler system the HRR drastically decreased (as well as battery surface temperatures, see further Appendix 2, Figure A1). One possible reason for the quickly declining HRR could possibly be attributed to that the rear window ruptured. This allowed water to reach to the interior of the vehicle, subsequently cooling the top of the battery, as seen by the battery surface temperature (ΔT ~ 796°). To eliminate the risk of having the sprinkler system active without having thermal runaway, it was decided to turn off the sprinkler system 10 min after activation.

After deactivation of the sprinkler system, a dry period of 15 min followed, where the fire was allowed to grow. A second activation of the sprinkler system was initiated after 15 min and it was left active for another 20 min in order to keep the water amount at

the same volume for all tests. During the second activation of the sprinkler system, thermal runaway was detected (Figure 6a).

The THR for the BEV was 5.7 GJ. The first two HRR peaks (0 – 60 min, sprinklers active) constituted of 27% of the THR, whereas the second peak (60 – 150 min) amounted to 73% of the THR (Figure 5c).

3.1.4 HRR Battery Test

For the free-standing battery the burner was centred underneath the battery pack. The time to initiate thermal runaway was substantially longer than for the BEV. After 60 min of testing, only minor venting events had been detected and it was decided to increase the burner output to 70 kW. The increased burner power immediately triggered thermal runaway in the battery and the burner output was immediately decreased to 30 kW again.

Since water was hindered to be directly applied on the battery pack, no cooling effect of the water on the battery was expected. The HRR graph for the battery test is presented in Figure 5d. The THR for the battery was 0.8 GJ.

The combustion of the battery lasted for 20 min. The combustion (and venting events) of the free-standing battery was visibly much more intense than for the BEV (Figure 6b). A plausible reason for this is that the gas vents and chassis were efficient in deflecting the jet flames underneath and towards the back of the vehicle. Additionally, the battery was burnt out in 20 min, whilst the BEV test continued for 150 min.

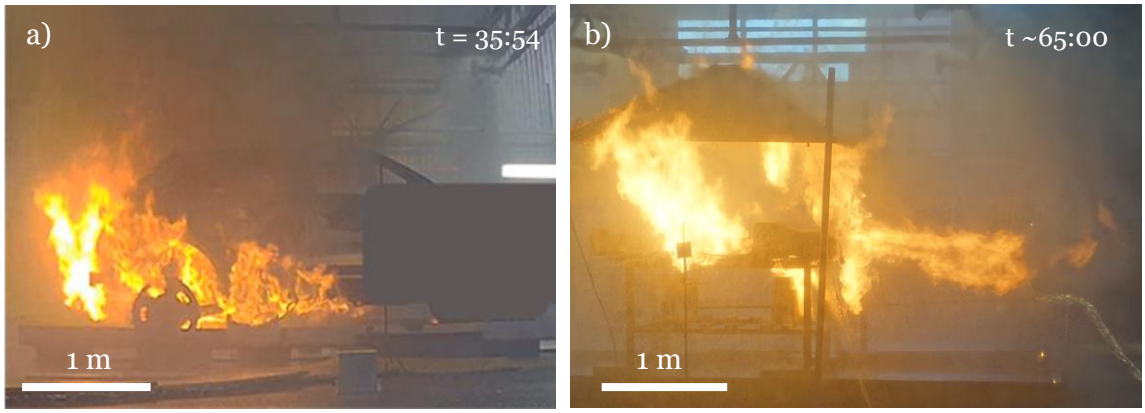

Figure 6. (a) Photograph of thermal runaway during the BEV test, in the second activation period of the sprinkler system and (b) photograph of thermal runaway during battery test.

3.2 Temperature Measurements

Temperature sensors placed in the vehicle and on the battery, as well as plate thermometers (PT) outside the vehicle, were used to monitor the temperature and heat radiation during the tests. Gas temperature graphs for all tests can be found in Appendix 2, Figure A1. Figure 7 presents the results from the PT placed outside the vehicle. These PT temperatures represent the actual heat exposure at the position and give an indication of the risk of fire propagation to adjacent vehicles with and without the sprinkler system activated.

In the reference test (free burning), the maximum PT temperature reached at 1 m from the vehicle was ~ 350°C (Figure 7a). At ~ 8 m the measured PT temperature was ~ 50°C. When the sprinkler system was active (for ICEV, BEV and battery), the PT temperature did not increase above ~ 80°C anywhere (Figure 7b-d). When the sprinklers were turned off, for the ICEV and BEV, the maximum PT temperature reached was ~ 200°C (Figure 7b-c).

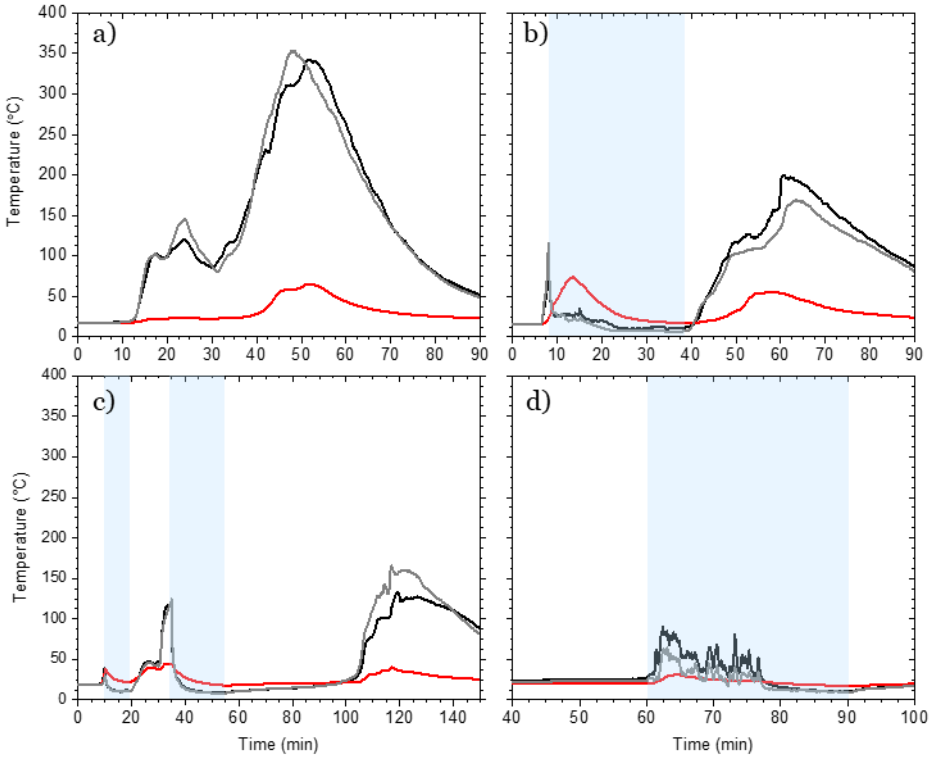

Figure 7. Temperatures measured using PT for (a) reference test, (b) ICEV, (c) BEV and (d) battery test. Black – left side of test object (distance 1 m), grey – right side of test object (distance 1 m) and red – behind test object (distance 8 m). Blue shading indicates the time when sprinklers were active. Note that the x-scale varies for a-d.

3.3 Gas Analysis

FTIR, FID and gas washing bottles (impinger sampling) were used to analyse the smoke collected in the duct. Time resolved FTIR and FID graphs for all tests can be found in Appendix 3 and 4.

The total amount of gaseous compounds detected by FTIR, impinger sampling, FID and through analysis of the FTIR pre-filter are presented in Table 7. Among the substances analysed, the major difference between the ICEV and BEV was the concentration of HF, similar to the results in [1]. The total amount of fluoride, chloride and bromide analysed for the impinger sampling, FTIR pre-filters and FTIR are presented in Table 8.

Table 7. Total amount of gaseous compounds for each test. Values in brackets represent the amount of analysed compound (mg) divided by the total mass loss of the vehicle/battery (g); values have been rounded

	Reference test	**ICEV**	**BEV**	**Battery**
		FTIR (g)		
CO_2	350 x 10^3 (1.5*)	435 x 10^3 (1.4*)	403 x 10^3 (1.2*)	72 x 10^3 (1.0*)
CO	7.7 x 10^3 (32)	9.9 x 10^3 (32)	9.9 x 10^3 (30)	1.2 x 10^3 (16)
HF	11 (0.05)	15 (0.05)	120 (0.4)	34 (0.5)
HCl	1 000 (4.2)	1 100 (3.6)	960 (2.9)	-
HBr	17 (0.07)	-	133 (0.4)	-
SO_2	1 600 (6.7)	1 700 (5.5)	700 (2.1)	260 (3.5)
HCN	110 (0.5)	70 (0.2)	40 (0.1)	1 (0.01)
NO	550 (2.3)	640 (2.1)	490 (1.5)	95 (1.3)
NO_2	55 (0.2)	130 (0.4)	40 (0.1)	2 (0.03)
NH_3	8 (0.03)	5 (0.02)	8 (0.02)	-
		FTIR pre-filter (g)		
F^-	30 (0.13)	25 (0.08)	120 (0.40)	260 (3.5)
Cl^-	40 (0.16)	60 (0.20)	40 (0.12)	10 (0.15)
Br^-	30 (0.13)	40 (0.13)	60 (0.18)	10 (0.14)
		Impinger sampling (g)		
F^-	140 (0.6)	80 (0.3)	270 (0.8)	240 (3.2)
Cl^-	960 (4)	1 100 (3.6)	1 350 (4.1)	30 (0.4)
Br^-	70 (0.3)	50 (0.2)	100 (0.3)	30 (0.4)
		FID (g)		
THC	2 260 (9.4)	5 960 (19.4)	5 120 (15.7)	996 (13.5)

*Value in gram per lost gram.
Values in red are below the limit of quantification (LOQ) for the FTIR analysis or due to noisy data which results in a large uncertainty.

3.3.1 Total Amount of HX from Gas Measurements

Table 8 presents the total amount of HX (HF, HCl and HBr) from the gas measurements, which includes FTIR and the FTIR pre-filter as well as the impinger sampling. Note, the impinger sampling and the FTIR pre-filters were analysed for ions (F^-, Cl^-, Br^-) and not for the acids (HCl, HF, HBr). However, for comparison, the amounts of fluoride, chloride and bromide captured by the gas washing bottles and in the pre-filters were recalculated to HF, HCl and HBr. These calculations will most likely lead to an overestimation of the concentration of HX.

The calculated total amount of HF for the reference vehicle, ICEV, BEV and battery was 40, 40, 240 and 290 g, respectively. Additionally, fluoride ions were also detected in the water samples; results are presented in section 3.4.

Table 8. Total amount of gaseous HX, based on FTIR + FTIR pre-filter analysis compared to ions collected through impinger sampling; values have been rounded

Reference test		ICEV	BEV	Battery
Calculated total amount of HX from FTIR + FTIR pre-filter (g)				
HF	40	40	240	290
HCl	1040	1160	1000	10
HBr	47	40	190	10
Calculated total amount of HX from impinger sampling (g)				
HF	140	80	270	240
HCl	960	1100	1350	30
HBr	70	50	100	30

FTIR Analysis during Water Application

Interestingly, using FTIR, no HF could be detected in the gas phase when the sprinkler system was active (Figure 8). Since the sprinkler system was active throughout the battery test, HF was not detected during the test using FTIR. However, 260 g of HF (recalculated from F^-) was found in the FTIR pre-filter. The reason that all the fluoride was found in the FTIR pre-filter need to be further investigated but highlights the importance of multiple measurement techniques to capture fluoride containing combustion products.

In the BEV fire test, HF was not detected using FTIR when the sprinklers were active. However, upon the second half of the test when the sprinklers were deactivated, HF could be detected (Figure 8a). Additionally, fluoride was detected in all tests by the gas washing bottles and in the FTIR pre-filter sampling. However, the impinger sampling and filter sampling are not time resolved measurements and can only detect ions.

Hydrochloric acid (HCl) was found in all vehicle tests using FTIR, with a total amount of ~ 1 000 g for each vehicle test. After the battery test, 30 g was found in the impinger bottles and 12 g HCl (recalculated from Cl^-) was found in the FTIR pre-filter, resulting in a total concentration of ~ 40 g for the battery test.

The THC content was found comparable for the ICEV and BEV fire test (Figure 9). For the reference test, the THC content was somewhat lower, probably due to the missing energy storage. Another reason that the THC content was higher for the sprinklered tests could be that these tests result in a higher degree of incomplete combustion products due to the lowered temperature. However, this hypothesis was not investigated further in this work.

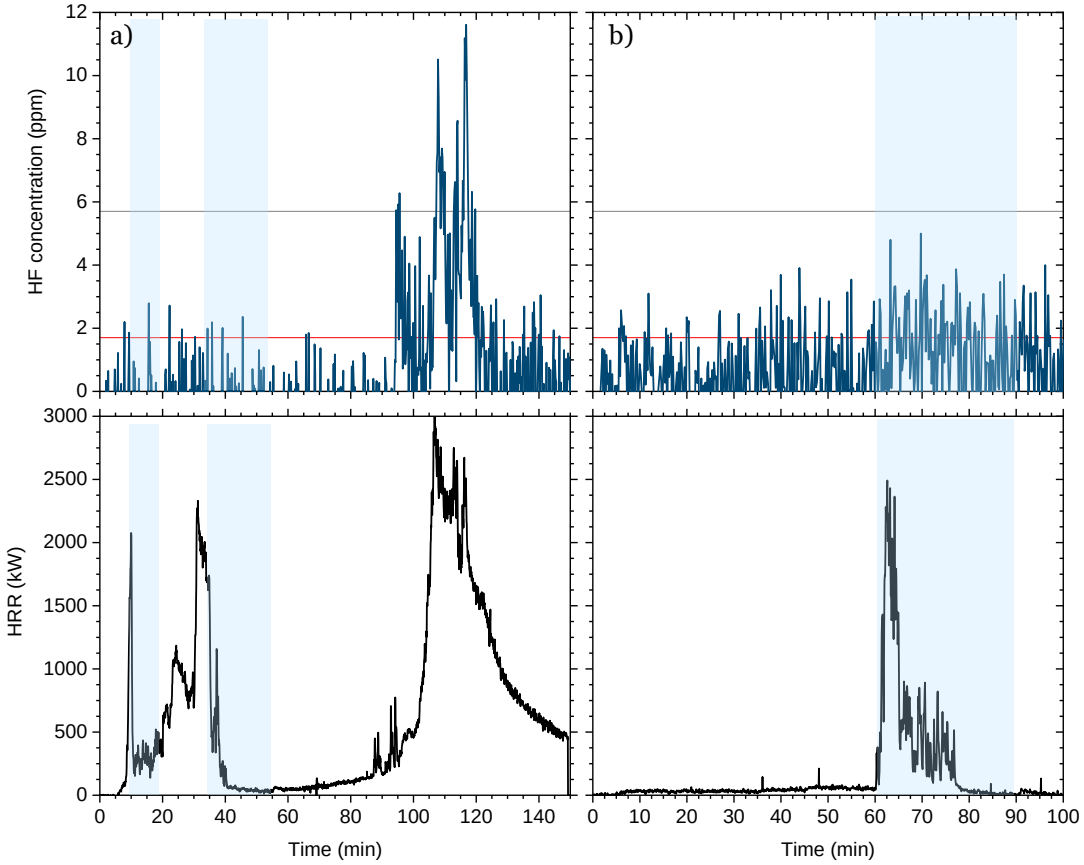

Figure 8. HF concentration measured using FTIR for (a) BEV and (b) battery test. Red line indicates minimum detection limit (MDL), and grey line indicates the LOQ. Below the FTIR graph, the corresponding HRR graph for each test is presented. Blue shading indicates the periods when the sprinkler system was active.

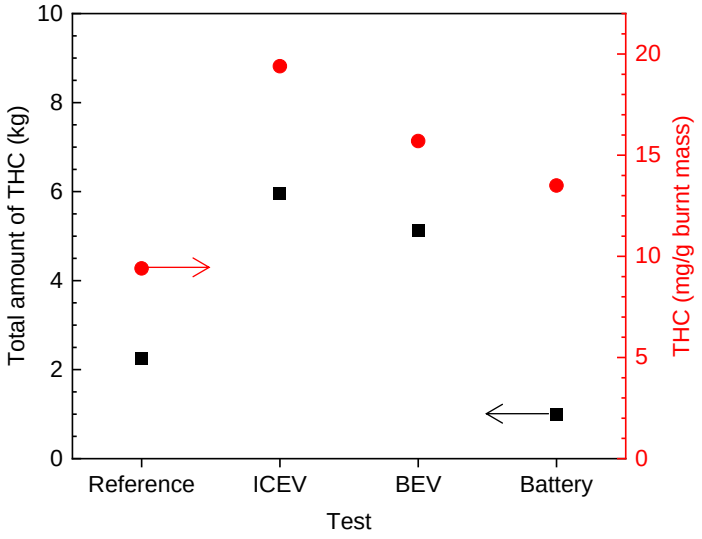

Figure 9. Total THC content in kilograms (black, left y-axis) and in mg per g mass burnt (red, right y-axis).

3.3.2 Soot Analysis

Values presented in Table 9 present the total amount of soot, metals/ions and PAHs analysed. Presented values are upscaled with the sampling factor between the quartz-filter sampling rate and the flow rate of the exhaust duct. Results for the metals/ions expressed in ppm of soot can be found in Appendix 4, Table A2.

The percentage of soot of the total mass burned (number presented in brackets in Table 9) decreases to half for the vehicle tests with sprinkler system activated compared to the free burning reference test. This indicates that potentially 50% or more (considering that the reference test lacked the energy storage) of the particulates for the vehicle tests are washed out by the sprinkler water.

For PAHs, the total amount was somewhat higher for the ICEV than for the BEV (Table 9). This is expected, as combustion of petrol may form a variety of the analysed PAHs. The battery contains a lower amount of organic matter and therefore released less PAHs compared to the ICEV. The total amount of PAHs for each test is presented in Table 9 and a detailed analysis of the different PAHs found from each test can be found in Appendix 6, Table A5.

Regarding the analysed metals and ions in soot, the total amount of aluminium, copper, cobalt, nickel, lithium, manganese and fluoride were substantially higher for the BEV and battery test compared to the ICEV and reference test. This was expected since the battery contains these metals and results are in line with our previous work. [1] For the tested ICEV, the amount of lead and zinc found in the soot is considerably higher compared to the other tests performed.

Table 9. Total amount of soot and metals/ions analysed from the quartz filters. Values in brackets represent the percentage of soot in comparison to the total mass loss of the vehicle/battery. Tabulated values have been rounded. Measurement error of ~ 10%

Compound	**Reference test**	**ICEV**	**BEV**	**Battery**
Soot (kg)	10 (4%)	6.5 (2%)	5.2 (2%)	2.8 (4%)
Total amount (g)				
Aluminium	-	7.0	90	165
Boron	-	-	-	-
Mercury	0.21	0.17	0.17	0.11
Lead	3.95	7.0	2.6	0.05
Cadmium	0.01	0.02	0.01	0.01
Cobalt	0.17	0.21	48	105
Nickel	1.25	0.90	258	555
Chromium	0.52	0.65	0.2	0.15
Copper	9.40	3.60	16.8	37
Tin	3.06	2.0	2.2	0.20
Vanadium	-	-	-	-
Zinc	130	99.0	47.8	7.2
Antimony	7.0	10.4	11.4	0.6
Arsenic	0.05	0.03	0.03	0.01
Lithium	-	-	50	155
Molybdenum	0.93	0.55	0.40	0.04

Compound	Reference test	ICEV	BEV	Battery
Manganese	0.5	0.5	40	89
Total amount (g)				
Fluoride	8.1	6.8	94.2	181
Chloride	140	96	65	4
Bromide	38	26	36	5.7
Total amount (g)				
PAHs	9.5	8.0	5.1	0.06
(-) indicate that the analysed compound was below the detection limit				

3.4 Extinguishing Water Analysis

Water samples were taken both from the pumped water (i.e. "time resolved" sampling) and from the large tray at the end of each test. Full results from the water analysis can be found in Appendix 5 and Appendix 6. Arsenic, cadmium, or mercury were not found in any of the water samples analysed in this study.

3.4.1 Analysis of Inorganics

Each analysed inorganic specie was compared to existing guideline values for surface water (some of which are found in Table 2) and are presented in Table 10. If the concentration of the analyte was higher than the guideline value, it is referred to as "above guideline value". However, no effects of dilution have been considered. Furthermore, the total volume of contaminants as well as the site of contamination needs to be assessed for a holistic view of the severity of pollutants. Note that some guideline values will vary depending on if it is salt or fresh water as the uptake (for some) of inorganic pollutants can be affected by water hardness and pH.

Table 10. Concentrations of analysed metals and ions in the 0 – 30 minutes sample in comparison to surface water guideline values

	Reference test	ICEV	BEV	Battery
Above GLV	-	Al, Cu, Co, Mo, Sb, Pb, Zn, F^-, Cl^-	Al, Cu, Co, Zn, Sb, F^-, Cl^-	Al, Cu, Co, Ni, F^-
Missing GLV	-	-	Li (30 mg L^{-1})	Li (110 mg L^{-1})
GLV – Guideline value				

Mercury, lead, cadmium and copper are often highlighted as the more severe environmental pollutants due to that they are bioaccumulating (valid for Hg, Pb, Cd) and highly toxic for aquatic organisms. Mercury and cadmium were not found in any of the analysed water samples. Lead was only found in the water from the ICEV (65 µg L^{-1}); the recommended guideline value for lead is 3 – 30 µg L^{-1}. Copper was found in all tests; the highest concentration of copper was found in the extinguishing water from the ICEV (90 µg L^{-1}) and then for the BEV (25 µg L^{-1}) and lastly the battery test (9 µg L^{-1}). The guideline value for copper in surface water range between 9 – 90 µg L^{-1}.

The surface water guideline values for chloride range between 120 – 640 mg L^{-1}. The analysed concentration of chloride range between 35 – 250 mg L^{-1}. This could potentially lead to harmful environmental effects, depending on the dilution and site of contamination. For fluoride, the recommended guideline values range between 0.12

[56] – 0.50 [56,60] mg L^{-1}. The fluoride concentrations in the analysed water ranged between 8 – 70 mg L^{-1}, well above the recommended values.

As of today, lithium has no established guideline value in Sweden. However, birth defects have been connected to a high lithium uptake in drinking water (>1 mg L^{-1}). [58] The EC_{50} varies depending on the organisms studied, but range between 1 – 197 mg L^{-1}. [59] The analysed water samples in this work contained 30 mg L^{-1} (BEV) and 110 mg L^{-1} (battery) of lithium. This could potentially influence aquatic life, depending on the dilution and site of contamination.

It was expected that the water samples taken after the tests would have contained higher concentrations of contaminants. The sprinkler system (for the vehicle tests) was active during the first half of the tests during which ~ 30% of the total heat was released. Additionally, the large tray was filled with varying amounts of debris from the burnt vehicles (molten metal, burnt plastic, cables, tire residues etc.) which metals/ions/compounds could bind to. However, analysis of the water samples showed that only six and nine, for the ICEV and BEV respectively, out of the 20 analysed compounds were found in higher concentrations after the test compared to the time resolved sampling. This might indicate that a vast amount of the inorganic species is washed away with the applied water.

The following compounds were found in higher concentration in the tray at the end of test compared to the time resolved sampling (0 – 30 min):

- ICEV: Co, Zn, Sb, Li, Cl^- and Br^-
- BEV: Al, B, Cr, V, Li, Mo, F^-, Cl^- and Br^-
- Battery: Al, B, Sb, Li, Mo, F^-, Cl^- and Br^-.

Copper was found in a lower amount in the battery test than in the background sample for the time resolved sampling (Appendix 5, table A3). This was probably due to that the copper in the previous test had not been completely flushed away when rinsing the setup after the BEV test (tray was only exchanged between the ICEV and BEV test).

Extrapolation of data to estimate the total concentration of detected species in water is not recommended due to the inhomogeneity of the concentrations of analyte upon testing. Even though sampling to some degree was time resolved, test heterogeneities will remain. Test heterogeneities is a result of a range of factors, such as the varying combustion behaviour with time, density of the smoke that the water penetrates, and how much of the water that is analysed, to mention a few.

Time Resolved Water Sampling of Fluoride

The BEV fire test had a total test time of 150 min. Out of these 150 min, the sprinkler system was active for 30 min (Figure 5). As presented in Table 11, the fluoride detected during the 30 min of sprinkler activation was quite low for the BEV compared to the battery test. However, the time resolved water sampling did not sample the full BEV fire, as the test prolonged for another 90 min after that the sprinkler system was turned off. In comparison to the BEV test, the battery test had a substantially shorter (more intense) burn time. The battery was consumed in ~ 20 min and the sprinkler system

was active throughout the test, resulting in higher concentrations of fluoride in the water samples compared to the BEV test.

Table 11. Time resolved fluoride analysis of all water samples from the BEV and battery test. Tabulated values have been rounded

Time	BEV	Battery
	mg L^{-1}	mg L^{-1}
0 – 10 min	0.2*	54
10 – 20 min	4.5	24
20 – 30 min	3.0	9.0
0 – 30 min	3.5	45
End of test	20	70
Blank test (background concentration): 0.05 to 0.3 mg L^{-1} fluoride *Value close to background concentration, most likely no (or very few) fluoride containing compounds were emitted from the battery during the first 10 min of sprinkler activation.		

The difference in the end concentration of fluoride, between the BEV and battery test, could potentially be a result of internal flushing of the battery pack after the test. The internal flushing was made to investigate if (or how much) the concentration of contaminants would increase in the extinguishing water upon flushing compared to the tested BEV (where the battery was not internally flushed). The fluoride concentration increased from 20 to 70 mg L^{-1} upon flushing the battery. Additionally, metals such as lithium, boron and aluminium were found in much higher concentrations in the extinguishing water upon flushing the battery, see further Appendix 5. A large increase in PFAS was also found, see further section 3.4.2.

3.4.2 Analysis of PFAS

PFAS was analysed for all water samples collected at the end of each test. The total amount of PFAS detected can be found in Table 12. A detailed analysis of each substance can be found in Appendix 6, Table A8.

The European Commission's limit values for PFAS in drinking water is 100 ng L^{-1} for PFAS 20 and 500 ng L^{-1} for PFAS total. Contaminated grounds at for example industrial sites and/or fire training areas may have PFAS concentrations of up to several thousands of µg per kg soil. In work by Brusseau et al., [65] data on soil concentrations of PFAS from all continents were aggregated. The maximum reported PFOS concentrations ranged upwards of several hundred mg kg^{-1}. In another study by Hepburn et al., [66] literature data of PFAS concentrations in ground water were summarised and showed concentrations ranging from 2 to over 300 000 ng L^{-1}.

For the reference test and the ICEV, the concentrations of PFAS are alike. However, for the BEV (test 3) the concentration of PFAS was somewhat lower (a factor of ~ 5 lower). The reason for this discrepancy is unknown and could potentially result from the measurement uncertainties for large-scale fire tests.

Additionally, flushing of the battery resulted in an increase of PFAS in the extinguishing water. As the battery pack included all electronics (cables, battery management system etc.) it is currently unclear if the increase in PFAS concentration stems from the battery cells, the electronics, or both and further tests are required to investigate the origin of the detected PFAS.

Firefighters that respond to vehicle fires should consider if flushing of the battery pack is necessary and if it can be done in a safe manner. The most environmental benign firefighting operation is one that uses less or no water. If an offensive tactic is necessary, collection of the extinguishing water could be used to hinder adverse environmental consequences.

Table 12. PFAS in extinguishing water analysed at the end of each test; tabulated values have been rounded. Measurement uncertainty ~ 30%

Blank samples	Reference test	ICEV	BEV	Battery (flushed)
Concentration, ng L^{-1} (ppt)				
60 – 100	1 300	860	200	4 700

3.4.3 Analysis of PAHs and VOCs

PAHs and VOCs in the sampled water were analysed using GC-MS and results in full can be found in Appendix 6.

Out of the 16 analysed PAHs, only six PAHs were found in the extinguishing water from the ICEV. From the BEV only two PAHs were found. The PAHs found were two- and three-ring PAHs. The total concentration of PAHs in the water samples was 12 and < 2.6 μg L^{-1} for the ICEV and the BEV, respectively. No PAHs were found in the extinguishing water from the battery fire test.

VOCs were only found in the water sample taken after the test for the ICEV, with a total concentration of ~ 2.6 mg L^{-1}. The following substances were found in majority: 1-(propan-2-yloxy)propan-2-one (580 μg L^{-1}), caprolactam (390 μg L^{-1}), phenol (370 μg L^{-1}), cyclopentanone (320 μg L^{-1}) and bisphenol A (220 μg L^{-1}).

3.4.4 Biological Characterisation

The criteria of acute toxicity for the evaluated microorganisms, presented in Table 13, are taken from the Swedish Environmental Protection Agency handbook. [67] All water samples tested had high or intermediate toxicity towards the tested aquatic species, Table 14.

In the Microtox analysis (*Vibrio fisheri*), the inhibition of bacteria luminescence (EC_{50} and EC_{20}) was measured. For 15 min of exposure, a vol/vol % of 0.35 to 0.75 (EC_{20}) and 1.8 to 4.0 (EC_{50}) was required which indicate that the tested extinguishing water had high toxicity towards *Vibrio fisheri*. Results are presented in Table 14.

For green algae (*Pseudokirchneriella subcapitata*), EC_{50} is presented in Table 14 (high toxicity for both samples). The no-observed-adverse-effect level (NOAEL) was 0.2 and 0.7 % vol/vol (72 h exposure) for ICEV and BEV, respectively.

For crustacean (*Daphnia magna*), EC_{50} is presented in Table 14 (high toxicity for ICEV and intermediate for BEV). The NOAEL 24 h exposure was 3.1 and 25 % vol/vol for ICEV and BEV, respectively. For a 48 h exposure, the NOAEL was 3.1 and 12.5 % vol/vol for ICEV and BEV, respectively.

Table 13. Criteria of acute toxicity based on EC_{50} taken from reference [67]

Effective concentration (% vol/vol)	**Level of toxicity**
> 100	Insignificant
70 – 100	Low
20 – 70	Intermediate
< 20	High

Table 14. Biological characterisation of extinguishing water. Tabulated values have been rounded. For the biological characterisation a lower value indicates a higher toxicity. The colour coding relates to the level of toxicity, see Table 13

	ICEV	**BEV**	**Battery**
pH	2.6 – 2.8	7.3 – 7.7	9.1
Salinity (‰)	0.5	0.3	0.3
Conductivity (mS cm^{-1})	2.6	7.5	9.1
Organism studied	Effective concentration (% vol/vol)		
Microtox (EC_{50}, 15 min)	1.8	3.5	4.0
Green algae (E_rC_{50}, 72 h)	2.5	6.5	Not tested
Crustacean (EC_{50}, 48 h)	14.0	30.5	Not tested
pH and salinity were adjusted according to the standardised protocols used			

pH and the effect on aquatic organisms

The ideal pH for most aquatic organisms falls between pH 6.5 - 8. EPA suggests a pH of 6.5 to 9 as water quality criteria in freshwater. [68] For many stream species, prolonged times of a pH below 5 will likely be lethal, resulting in significant changes in species composition and diversity. Short-term exposures of fish to high pH (above ~ 9.5) are seldom lethal. However, persistent exposure to pH between 9.5 and 10 can damage for example gills, eyes, and skin. [68] High pH can also contribute to ammonia toxicity since the ionized form (NH_4^+) will form ammonia (NH_3), as the pH increases. [68]

Interestingly, the pH of the extinguishing water resulting from the BEV and battery testing is remarkably different to the pH for the ICEV test (Table 14). For the BEV test, the water had a pH of 7.3 – 7.7, which is near neutral pH (pH 7.0). The water sampled from the battery test was alkaline (pH 9.1) whilst the water from the ICEV was acidic, pH 2.6 – 2.8. The reason for variations in pH for the water taken after the BEV fire test (or alkaline pH for the battery test) has not been investigated further but could be due to the carbonate chemistries used in LIBs. The difference in pH could potentially play a role for the environmental consequences. The results from the biological characterisation have not been affected by the varying pH since the tested samples were buffered before analysis.

4 Conclusions

In a previous project by RISE called *Toxic gases from fire in electric vehicles* [1] (funded by the Swedish Energy Agency, No. 48193-1), hydrogen fluoride, nickel, cobalt, lithium and manganese were found in higher concentration from BEV fire compared to an ICEV fire. This was confirmed by the current work. Additionally, the extinguishing water from the BEV and the battery pack contained higher concentrations of lithium and fluoride than the extinguishing water from the ICEV. Lithium has no surface water guideline in Sweden, whereas fluoride is toxic to water living organisms at the found concentrations (dilution effects not considered).

For the ICEV, lead was found in much higher concentrations than for the BEV. Lead was found for the ICEV test both in the combustion gases as well as in the extinguishing water. Furthermore, PAHs and VOCs were found to a higher degree for the ICEV than for the BEV.

The concentration of PFAS in the extinguishing water was 200 and 860 ng L^{-1} for the BEV and ICEV, respectively. After the battery pack test, the pack was opened and flushed with tap water. Flushing of the battery pack (including cells and electronics) increased the concentration of PFAS to 4 700 ng L^{-1}. Further studies are required to investigate the origin of these PFAS, as they could derive from the battery cells or/and the electronic components found in the battery pack. Many of the fluorinated compounds used in LIBs improve the performance and lifetime of LIBs. Therefore, substitution of these compounds, without having deteriorating performances of the LIB, may be difficult. Firefighters that respond to BEV fires should consider if flushing of the battery is necessary. If it is necessary, it should be performed in a safe manner, to avoid pollution to the environment. In some cases, the most environmental benign firefighting tactic could be to not extinguish the fire at all. For sites where many batteries are stored, for example large stationary battery storages or warehouses, preventive measures to reduce serious harm of extinguishing water contamination could be necessary. One way of doing this is to build structures that can redirect or contain extinguishing water if needed.

Additionally, flushing of the battery increased the concentration of aluminium, lithium and fluoride by a factor of 6, 3 and 7 respectively, compared to the BEV.

The biological characterisation indicates that all extinguishing water analysed in this work were toxic towards the tested aquatic species. The analysed extinguishing water from the ICEV had somewhat higher toxicity to the tested aquatic species than the extinguishing water from the BEV. Additionally, the extinguishing water from the ICEV had a low pH ~ 2.7, whereas the extinguishing water from the BEV had a near neutral pH of ~ 7.5.

Nevertheless, each polluting scenario needs to be assessed individually and effects of dilution needs to be considered to fully evaluate the severeness of pollution. Additionally, the sensitivity to each pollutant will differ depending on the recipient, which also needs to be considered. The analysed compounds presented in this report are only representative for a small number of tests. As vehicle type, battery chemistry, fire scenario etc. are varied, the pollutants and concentrations of these will be subjected to variations.

References

[1] O. Willstrand, R. Bisschop, A. Temple, J. Anderson, Toxic Gases from Fire in Electric Vehicles, 2020. http://urn.kb.se/resolve?urn=urn:nbn:se:ri:diva-52000 (accessed May 5, 2022).

[2] A. Lönnermark, P. Blomqvist, Emissions from an automobile fire, Chemosphere. 62 (2006) 1043–1056. https://doi.org/10.1016/j.chemosphere.2005.05.002.

[3] N. Watanabe, O. Sugawa, T. Suwa, Y. Ogawa, M. Hiramatsu, H. Tomonori, H. Miyamoto, K. Okamoto, M. Honma, Comparison of fire behaviors of an electric-battery-powered vehicle and gasoline-powered vehicle in a real-scale fire test, in: P. Andersson, B. Sundström (Eds.), Fires in Vehicles - FIVE 2016, SP, Borås, 2016: pp. 195–206. http://urn.kb.se/resolve?urn=urn:nbn:se:ri:diva-30071.

[4] C. Lam, D. MacNeil, R. Kroeker, G. Lougheed, G. Lalime, Full-Scale Fire Testing of Electric and Internal Combustion Engine Vehicles, in: P. Andersson, B. Sundström (Eds.), Fires in Vehicles - FIVE 2016, Baltimore, 2016: pp. 95–106. https://ri.diva-portal.org/smash/get/diva2:1120218/FULLTEXT01.pdf (accessed January 12, 2022).

[5] B. Truchot, F. Fouillen, S. Collet, An experimental evaluation of toxic gas emissions from vehicle fires, Fire Saf J. 97 (2018) 111–118. https://doi.org/10.1016/j.firesaf.2017.12.002.

[6] A. Lecocq, M. Bertana, B. Truchot, G. Marlair, Comparison of the fire consequences of an electric vehicle and an internal combustion engine vehicle, in: International Conference on Fires In Vehicles - FIVE 2012, Chicago, 2012: pp. 183–194. https://hal-ineris.archives-ouvertes.fr/ineris-00973680/document (accessed January 12, 2022).

[7] E. Emilsson, L. Dahllöf, M. Ljunggren Söderman, Plastics in passenger cars, Stockholm, 2019. https://www.ivl.se/download/18.14d7b12e16e3c5c36271082/1574935157259/C454.pdf (accessed May 5, 2022).

[8] T.R. Hull, K.T. Paul, Bench-scale assessment of combustion toxicity—A critical analysis of current protocols, Fire Saf J. 42 (2007) 340–365. https://doi.org/10.1016/J.FIRESAF.2006.12.006.

[9] J. Finkelstein, D. Frankel, J. Noffsinger, Fully decarbonizing the power industry, 2020.

[10] A.A. Tidblad, K. Edström, G. Hernández, I. de Meatza, I. Landa-Medrano, J. Jacas Biendicho, L. Trilla, M. Buysse, M. Ierides, B.P. Horno, Y. Kotak, H.-G. Schweiger, D. Koch, B.S. Kotak, Future Material Developments for Electric Vehicle Battery Cells Answering Growing Demands from an End-User Perspective, Energies (Basel). 14 (2021) 4223. https://doi.org/10.3390/en14144223.

[11] M. Armand, P. Axmann, D. Bresser, M. Copley, K. Edström, C. Ekberg, D. Guyomard, B. Lestriez, P. Novák, M. Petranikova, W. Porcher, S. Trabesinger, M. Wohlfahrt-Mehrens, H. Zhang, Lithium-ion batteries – Current state of the art and anticipated developments, J Power Sources. 479 (2020) 228708. https://doi.org/10.1016/j.jpowsour.2020.228708.

[12] J.W. Fergus, Ceramic and polymeric solid electrolytes for lithium-ion batteries, J Power Sources. 195 (2010) 4554–4569. https://doi.org/10.1016/J.JPOWSOUR.2010.01.076.

[13] F. Zheng, M. Kotobuki, S. Song, M.O. Lai, L. Lu, Review on solid electrolytes for all-solid-state lithium-ion batteries, J Power Sources. 389 (2018) 198–213. https://doi.org/10.1016/J.JPOWSOUR.2018.04.022.

[14] X. Feng, M. Ouyang, X. Liu, L. Lu, Y. Xia, X. He, Thermal runaway mechanism of lithium ion battery for electric vehicles: A review, Energy Storage Mater. 10 (2018) 246–267. https://doi.org/10.1016/J.ENSM.2017.05.013.

[15] X. Liu, D. Ren, H. Hsu, X. Feng, G.L. Xu, M. Zhuang, H. Gao, L. Lu, X. Han, Z. Chu, J. Li, X. He, K. Amine, M. Ouyang, Thermal Runaway of Lithium-Ion Batteries without Internal Short Circuit, Joule. 2 (2018) 2047–2064. https://doi.org/10.1016/J.JOULE.2018.06.015.

[16] G. Zhang, X. Wei, X. Tang, J. Zhu, S. Chen, H. Dai, Internal short circuit mechanisms, experimental approaches and detection methods of lithium-ion batteries for electric vehicles: A review, Renewable and Sustainable Energy Reviews. 141 (2021) 110790. https://doi.org/10.1016/J.RSER.2021.110790.

[17] Z. Wang, D. Ouyang, • Mingyi Chen, • Xuehui Wang, Z. Zhang, J. Wang, Fire behavior of lithium-ion battery with different states of charge induced by high incident heat fluxes, (n.d.). https://doi.org/10.1007/s10973-018-7899-y.

[18] F. Larsson, P. Andersson, P. Blomqvist, A. Lorén, B.E. Mellander, Characteristics of lithium-ion batteries during fire tests, J Power Sources. 271 (2014) 414–420. https://doi.org/10.1016/J.JPOWSOUR.2014.08.027.

[19] P. Ribière, S. Grugeon, M. Morcrette, S. Boyanov, S. Laruelle, G. Marlair, Investigation on the fire-induced hazards of Li-ion battery cells by fire calorimetry, Energy Environ. Sci. 5 (2012) 5271–5280. https://doi.org/10.1039/C1EE02218K.

[20] G. Zhong, B. Mao, C. Wang, L. Jiang, K. Xu, J. Sun, Q. Wang, Thermal runaway and fire behavior investigation of lithium ion batteries using modified cone calorimeter, (n.d.). https://doi.org/10.1007/s10973-018-7599-7.

[21] H. Li, Q. Duan, C. Zhao, Z. Huang, Q. Wang, Experimental investigation on the thermal runaway and its propagation in the large format battery module with Li(Ni1/3Co1/3Mn1/3)O2 as cathode, J Hazard Mater. 375 (2019) 241–254. https://doi.org/10.1016/J.JHAZMAT.2019.03.116.

[22] Q. Wang, B. Mao, S.I. Stoliarov, J. Sun, A review of lithium ion battery failure mechanisms and fire prevention strategies, Prog Energy Combust Sci. 73 (2019) 95–131. https://doi.org/10.1016/j.pecs.2019.03.002.

[23] J. Lamb, C.J. Orendorff, E.P. Roth, J. Langendorf, Studies on the Thermal Breakdown of Common Li-Ion Battery Electrolyte Components, J Electrochem Soc. 162 (2015) A2131–A2135. https://doi.org/10.1149/2.0651510jes.

[24] B. Ravdel, K.M. Abraham, R. Gitzendanner, J. DiCarlo, B. Lucht, C. Campion, Thermal stability of lithium-ion battery electrolytes, J Power Sources. 119–121 (2003) 805–810. https://doi.org/10.1016/S0378-7753(03)00257-X.

[25] J.S. Gnanaraj, E. Zinigrad, L. Asraf, H.E. Gottlieb, M. Sprecher, M. Schmidt, W. Geissler, D. Aurbach, A Detailed Investigation of the Thermal Reactions of LiPF[sub 6] Solution in Organic Carbonates Using ARC and DSC, J Electrochem Soc. 150 (2003) A1533. https://doi.org/10.1149/1.1617301.

[26] F. Baakes, M. Lüthe, M. Gerasimov, V. Laue, F. Röder, P.B. Balbuena, U. Krewer, Unveiling the interaction of reactions and phase transition during thermal abuse of Li-ion batteries, J Power Sources. 522 (2022) 230881. https://doi.org/https://doi.org/10.1016/j.jpowsour.2021.230881.

[27] P. Ping, Q.S. Wang, P.F. Huang, K. Li, J.H. Sun, D.P. Kong, C.H. Chen, Study of the fire behavior of high-energy lithium-ion batteries with full-scale burning test, J Power Sources. 285 (2015) 80–89. https://doi.org/10.1016/J.JPOWSOUR.2015.03.035.

[28] World Health Organization, Air Quality Guidelines Global Update 2005, Copenhagen, 2006.

[29] K.H. Kim, S.A. Jahan, E. Kabir, R.J.C. Brown, A review of airborne polycyclic aromatic hydrocarbons (PAHs) and their human health effects, Environ Int. 60 (2013) 71–80. https://doi.org/10.1016/J.ENVINT.2013.07.019.

[30] H. Zhang, X. Zhang, Y. Wang, P. Bai, K. Hayakawa, L. Zhang, N. Tang, Characteristics and Influencing Factors of Polycyclic Aromatic Hydrocarbons Emitted from Open Burning and Stove Burning of Biomass: A Brief Review, Int J Environ Res Public Health. 19 (2022) 3944. https://doi.org/10.3390/ijerph19073944.

[31] D.M. Pinto, J.D. Blande, S.R. Souza, A.-M. Nerg, J.K. Holopainen, Plant Volatile Organic Compounds (VOCs) in Ozone (O3) Polluted Atmospheres: The Ecological Effects, J Chem Ecol. 36 (2010) 22–34. https://doi.org/10.1007/s10886-009-9732-3.

[32] P. Sicard, A. Anav, A. de Marco, E. Paoletti, Projected global ground-level ozone impacts on vegetation under different emission and climate scenarios, Atmos Chem Phys. 17 (2017) 12177–12196. https://doi.org/10.5194/acp-17-12177-2017.

[33] J. Briffa, E. Sinagra, R. Blundell, Heavy metal pollution in the environment and their toxicological effects on humans, Heliyon. 6 (2020) e04691. https://doi.org/https://doi.org/10.1016/j.heliyon.2020.e04691.

[34] A. Rensmo, Per- and Polyfluoroalkyl Substances (PFAS) Emissions from Recycling Processes of Lithium-Ion Batteries, 2022. http://urn.kb.se/resolve?urn=urn:nbn:se:uu:diva-479345 (accessed July 4, 2022).

[35] X. Hu, E. Mousa, L. Ånnhagen, Z. Musavi, M. Alemrajabi, B. Hall, G. Ye, Complex gas formation during combined mechanical and thermal treatments of spent lithium-ion-battery cells, J Hazard Mater. 431 (2022) 128541. https://doi.org/https://doi.org/10.1016/j.jhazmat.2022.128541.

[36] D. Mckee, A. Thoma, K. Bailey, J. Fish, a review of hydrofluoric acid burn management, 2014.

[37] H. Wingfors, R. Magnusson, L. Thors, M. Thunell, Gasformig HF vid brand i trånga utrymmen-risker för hudupptag vid insatser, 2021. https://rib.msb.se/filer/pdf/29507.pdf (accessed January 12, 2022).

[38] K. Dennerlein, F. Kiesewetter, S. Kilo, T. Jäger, T. Göen, G. Korinth, H. Drexler, Dermal absorption and skin damage following hydrofluoric acid exposure in an ex vivo human skin model, Toxicol Lett. 248 (2016) 25–33. https://doi.org/10.1016/j.toxlet.2016.02.015.

[39] AISAB, Prehospital förmåga vid insatser med bränder i litiumjonbatterier, (2021). https://www.youtube.com/watch?v=vaspu8f_X_w (accessed January 12, 2022).

[40] EPA, Acute exposure guideline levels for selected airborn chemicals, 2004. https://www.epa.gov/sites/default/files/2014-11/documents/tsd53.pdf (accessed March 30, 2022).

[41] F. Larsson, P. Andersson, B.-E. Mellander, Toxic fluoride gas emissions from lithium-ion battery fires, (n.d.). https://doi.org/10.1038/s41598-017-09784-z.

[42] G. Lombardo, B. Ebin, M.R. Mark, B.M. Steenari, M. Petranikova, Incineration of EV Lithium-ion batteries as a pretreatment for recycling – Determination of the potential formation of hazardous by-products and effects on metal compounds, J Hazard Mater. 393 (2020). https://doi.org/10.1016/j.jhazmat.2020.122372.

[43] F. Amon, J. Gehandler, R. Mcnamee, M. Mcnamee, A. Vilic, Measuring the impact of fire on the environment (Fire Impact Tool, version 1) Project report and user manual, 2019. https://doi.org/10.23699/tmpv-pj71.

[44] A. Kärrman, F. Bjurlid, J. Hagberg, N. Ricklund, M. Larsson, J. Stubleski, H. Hollert, Study of environmental and human health impacts of firefighting agents : A technical report, Örebro University, Örebro, Sweden, 2016. http://urn.kb.se/resolve?urn=urn:nbn:se:oru:diva-54919.

[45] J. Fowles, M. Person, D. Noiton, The ecotoxicity of fire-water runoff. Part one: Review of litterature, 2001.

[46] Naturvårdsverket, Metodik för inventering av förorenade områden, 1999.

[47] D. Martin, M. Tomida, B. Meacham, Environmental impact of fire, Fire Sci Rev. 5 (2016) 5. https://doi.org/10.1186/s40038-016-0014-1.

[48] EPA, Aquatic life ambient water quality criteria for aluminum in freshwater, Washington, 2018. https://www.federalregister.gov/documents/2018/12/21/2018-27745/aquatic-life-ambient-water-quality-criteria-for-aluminum-in-freshwater (accessed April 6, 2022).

[49] Canadian Environmental Protection Act, 1999 - Federal environmental quality guidelines - aluminium, (2021) 1–17. https://www.canada.ca/en/environment-climate-change/services/evaluating-existing-substances/federal-environmental-quality-guidelines-aluminium.html (accessed April 6, 2022).

[50] CCME, Canadian water quality guidelines for the protection of aquatic life: Boron, (2009) 1–9. https://www.ccme.ca/en/res/boron-en-canadian-water-quality-guidelines-for-the-protection-of-aquatic-life.pdf (accessed April 6, 2022).

[51] N.K. Nagpal, Technical report - Water quality guidelines for cobalt, Victoria BC, 2004.

[52] CCME, Water quality guidelines for the protection of agriculture: Lithium, (1999). https://www.ccme.ca/en/chemical/127#_ag_irrigation_concentration (accessed April 6, 2022).

[53] CCME, Canadian water quality guidelines for the protection of aquatic life: Manganese, (2019). https://www.ccme.ca/en/res/manganese-en-canadian-water-quality-guidelines-for-the-protection-of-aquatic-life.pdf (accessed April 6, 2022).

[54] CCME, Canadian water quality guidelines for the protection of aquatic life: Molybdenum, (1999) 1–4. https://www.ccme.ca/en/res/molybdenum-en-canadian-water-quality-guidelines-for-the-protection-of-aquatic-life.pdf (accessed April 6, 2022).

[55] CCME, Canadian water quality guidelines for the protection of aquatic life: Chloride, (2011) 1–16. https://www.ccme.ca/en/res/chloride-en-canadian-water-quality-guidelines-for-the-protection-of-aquatic-life.pdf (accessed April 6, 2022).

[56] CCME, Canadian water quality guidelines for the protection of aquatic life: Inorganic Fluorides, (1999) 1–4. https://www.ccme.ca/en/res/fluorides-inorganic-en-canadian-water-quality-guidelines-for-the-protection-of-aquatic-life.pdf (accessed April 6, 2022).

[57] G.N. Schrauzer, Lithium: Occurrence, Dietary Intakes, Nutritional Essentiality, J Am Coll Nutr. 21 (2002) 14–21. https://doi.org/10.1080/07315724.2002.10719188.

[58] F. Harari, L. Maxe, M. Vahter, Lithium, boron, cesium and other potentially toxic metals in swedish well water, Stockholm, 2017. https://ki.se/media/233484/download?attachment (accessed October 17, 2022).

[59] H. Aral, A. Vecchio-Sadus, Toxicity of lithium to humans and the environment—A literature review, Ecotoxicol Environ Saf. 70 (2008) 349–356. https://doi.org/https://doi.org/10.1016/j.ecoenv.2008.02.026.

[60] J.A. Camargo, Fluoride toxicity to aquatic organisms: a review, Chemosphere. 50 (2003) 251–264. https://doi.org/10.1016/S0045-6535(02)00498-8.

[61] G. Dave, Effects of fluoride on growth, reproduction and survival in Daphnia magna, Comparative Biochemistry and Physiology Part C: Comparative Pharmacology. 78 (1984) 425–431. https://doi.org/https://doi.org/10.1016/0742-8413(84)90110-5.

[62] R. Kühn, M. Pattard, K.D. Pernak, A. Winter, Results of the harmful effects of water pollutants to Daphnia magna in the 21 day reproduction test, Water Res. 23 (1989) 501–510. https://doi.org/10.1016/0043-1354(89)90142-5.

[63] SGU, Geological Survey of Sweden - Geomap, (n.d.). https://www.sgu.se/en/products/maps/geomap/ (accessed January 18, 2022).

[64] T.R. Long, A.F. Blum, T.J. Bress, B.R.T. Cotts, Best Practices for Emergency Response to Incidents Involving Electric Vehicles Battery Hazards: A Report on Full-Scale Testing Results, 2013. https://www.energy.gov/sites/prod/files/2014/02/f8/final_report_nfpa.pdf (accessed January 18, 2022).

[65] M.L. Brusseau, R.H. Anderson, B. Guo, PFAS concentrations in soils: Background levels versus contaminated sites, Science of The Total Environment. 740 (2020) 140017. https://doi.org/10.1016/J.SCITOTENV.2020.140017.

[66] E. Hepburn, C. Madden, D. Szabo, T.L. Coggan, B. Clarke, M. Currell, Contamination of groundwater with per- and polyfluoroalkyl substances (PFAS) from legacy landfills in an urban re-development precinct, Environmental Pollution. 248 (2019) 101–113. https://doi.org/10.1016/J.ENVPOL.2019.02.018.

[67] Naturvårdsverket, Handbok 2010:3 Kemisk och biologisk karakterisering av punktutsläpp till vatten, 2011.

[68] United States Environmental Protection Agency (EPA), CADDIS Volume 2: pH, (n.d.). https://www.epa.gov/caddis-vol2/ph (accessed October 17, 2022).

Appendix 1: Fluorinated compounds found in LIBs

Table A1. Summary of common fluorinated components in LIBs, state-of-the-art materials are highlighted in bold. Table taken from reference [34].

Function	Chemical name	Abbreviation
Binder	**poly(vinylidene fluoride)**	**PVDF**
	poly(vinylidene fluoride co-hexafluoropropylene)	P(VDF-HFP)
	poly(vinylidene fluoride-co-trifluoroethylene)	P(VDF-TrFE)
	poly(tetrafluoroethylene)	PTFE
	fluorinated ethylene propylene	FEP
	Fluoro acrylic polymer	TRD202A
Separator	poly(vinylidene fluoride)	PVDF
	poly(vinylidene fluoride co-hexafluoropropylene)	PVDF-HFP
Electrode surface	aluminium fluoride	AlF_3
Electrolyte, salt	**lithium hexafluorophosphate**	**$LiPF_6$**
	lithium hexafluoroarsenate	$LiAsF_6$
	lithium tetraborate	$LiBF_4$
	lithium bis(trifluoromethylsulfoyl)imide	LiTFSI
	lithium bis(perfluoroethanesulfonyl)imide	LiBETI
	lithium difluoro(oxalate)borate	LiDFOB
	lithium bis(fluorosulfonyl)imide	LiFSI
	lithium fluorosulfonyl-trifluorofulfonyl imide	LiFTFSI
	lithium fluoroalkyl phosphatelithium	LiFAP
	lithium trifluoromethanesulfonate	Triflate
Electrolyte, solvent	fluoroethylene carbonate	FEC
	difluoroethylene carbonate	DFEC
	trifluoropropylene carbonate	TFPC
	methyl difluoroacetate	MDFA
	tetrafluoroethyl-tetrafluoropropyl ether	F-EPE

Appendix 2: Gas temperature graphs

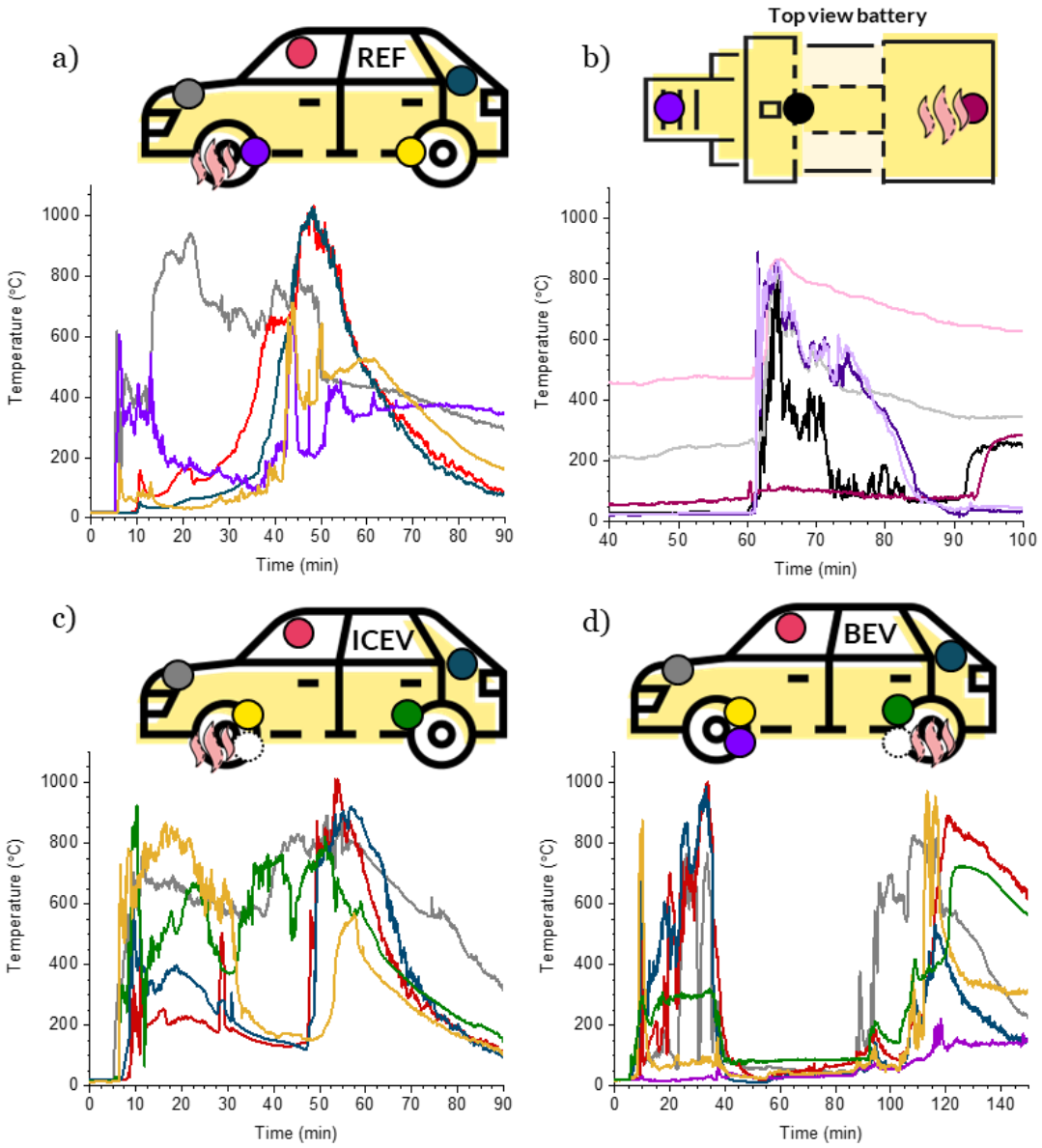

Figure A1. Gas temperature graphs for (a) reference, (b) battery, (c) ICEV and (d) BEV fire tests. Burner was ignited at 5 min for all tests. Color-coding can be seen in the sketch above each graph, where each coloured circle represents a temperature sensor. Sensors were placed centred in the vehicle. For the vehicle tests the yellow, green and purple sensors are placed on/under the tank/battery. The white circles indicate sensors that were placed in close vicinity to the burner and are therefore not presented in the graphs as temperatures only represent the burner temperature. Pink flames represents the burner placement. For (b) lighter shading indicate sensors placed on the bottom side of the battery. For the ICEV test (c) sprinklers were active, t ~ 09:30 to 29:30 min, for BEV test (d) sprinklers were active t ~ 09:50 to 19:50 and 34:50 to 54:50 min.

Appendix 3: Gas analysis - FTIR spectroscopy

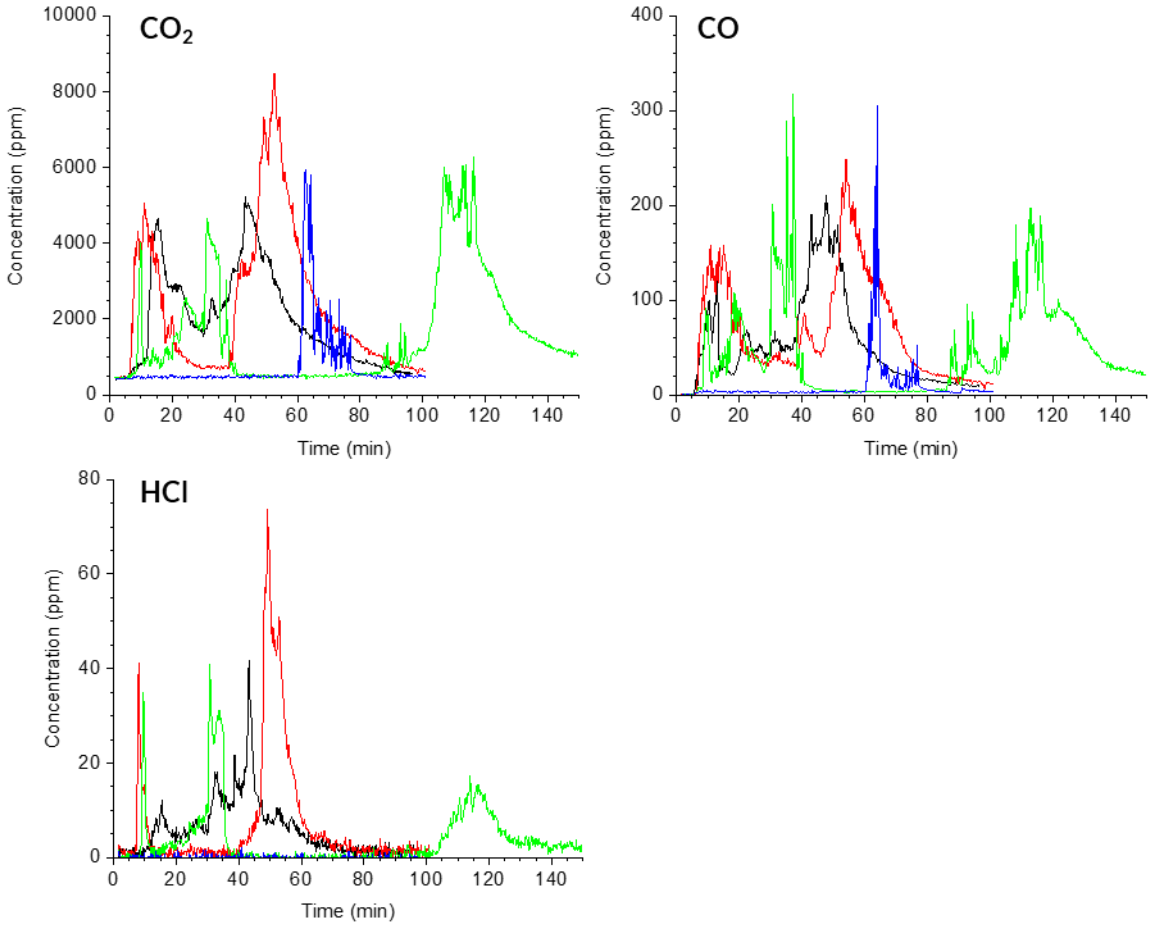

Figure A2. FTIR measurements of CO_2, CO, and HCl. Black – reference, Red – ICEV, Green – BEV, and Blue – Battery. Note that the y-scales have different grading and that HCl was not detected for the battery test using FTIR.

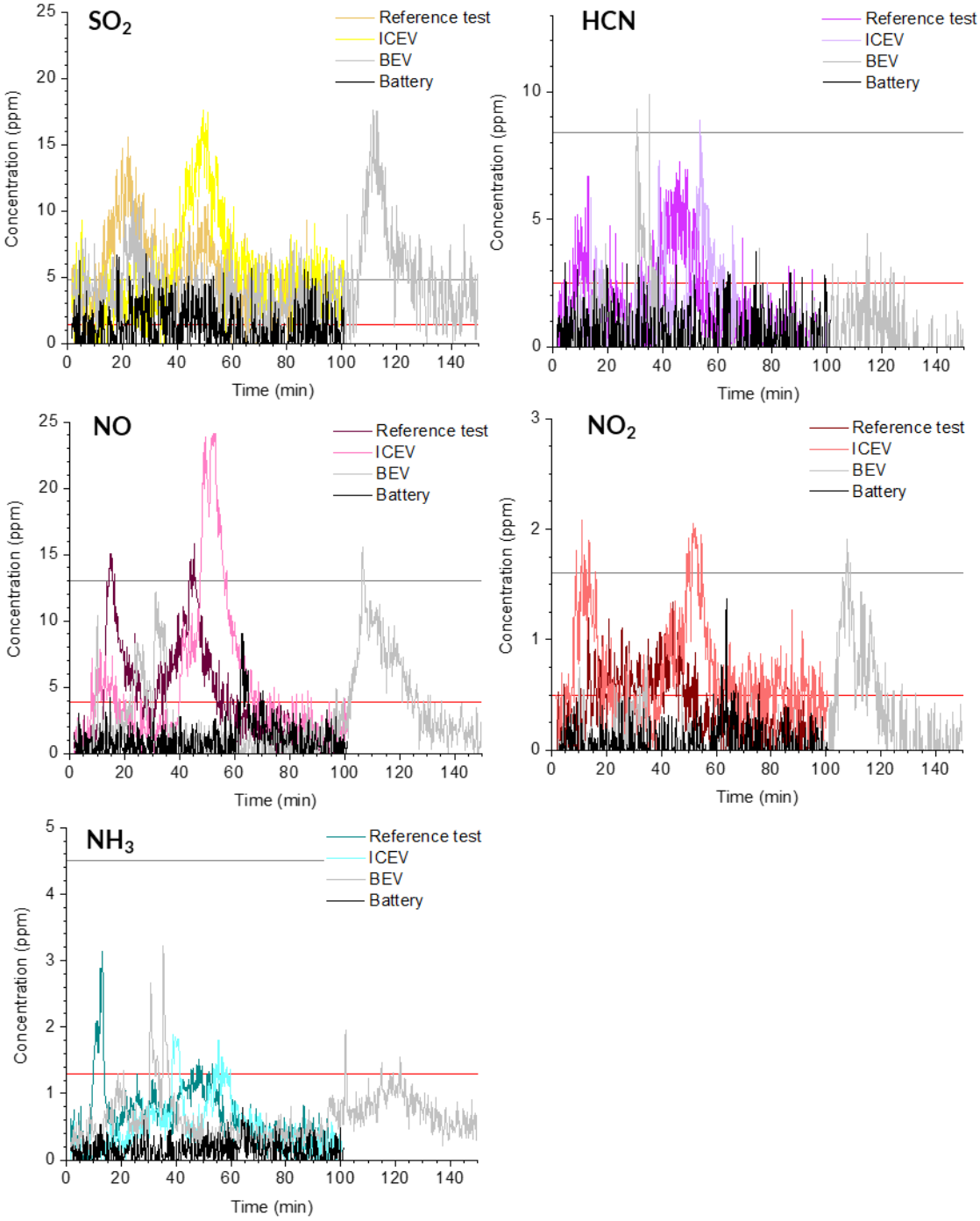

Figure A3. FTIR measurements of SO_2, HCN, NO, NO_2 and NH_3. Grey line indicates "*limit of quantification*" (LOQ), and red line indicates "*minimum detection limit*" (MDL). Graph legend provide test object. Note that the *y-scales* have different scaling.

Appendix 4: Soot analysis

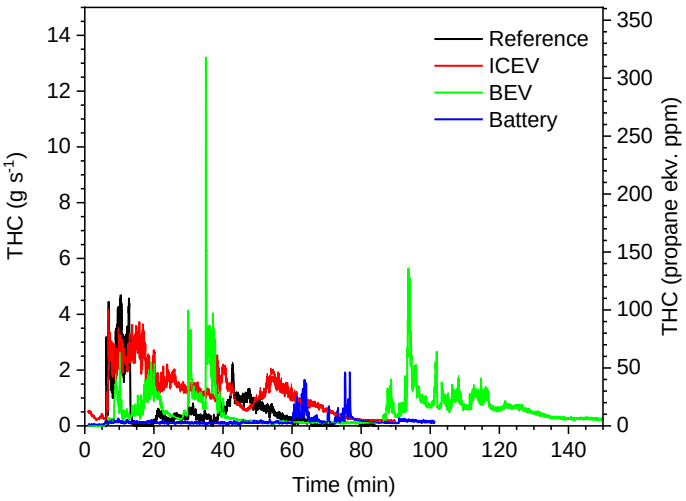

Figure A4. Total hydrocarbon content (THC) in grams per second (left y-axis) and in parts per million (ppm) propane equivalents (right y-axis) measured using FID.

Table A2. Metals and ions from quartz filter in the exhaust duct. Number in brackets for the soot is the percentage of soot of the total mass lost. Results for the metals/ions are expressed as parts per million (ppm) of soot, values have been rounded. Measurement uncertainty ± ~ 10%

	Reference test	ICEV	BEV	Battery
Soot (kg)	10 (4)	6.5 (2.1)	5.2 (1.6)	2.8 (3.8)
Ratio against soot (ppm)				
Aluminium	-	1050	17000	44000
Boron	-	-	-	-
Mercury	23	26	33	29
Lead	425	1047	510	14
Cadmium	1.5	2.5	2.5	2.5
Cobalt	18	31	9500	28000
Nickel	133	134	51000	150000
Chromium	56	97	41	40
Copper	1000	540	3320	9975
Tin	328	300	434	55
Vanadium	-	-	-	-
Zinc	14000	14800	9500	1950
Antimony	750	1550	2200	170
Arsenic	5	5	6	3
Lithium	-	-	9960	41900
Molybdenum	100	82	76	10
Manganese	50	73	7920	24000
Fluoride	810	1050	18000	65000
Chloride	14000	15000	12500	1400
Bromide	3900	4100	6900	2000
(–) below detection limit				

Appendix 5: Water sampling of metals and ions

Table A3. Metal and ion content of water samples (time resolved sample, 0 – 30 min). Numbers in brackets indicate the error of the measurement obtained from blank test. All tabulated values have been rounded. Measurement uncertainty ± ~ 10%

Compound	Reference test*	ICEV	BEV	Battery
Concentration (mg L^{-1})				
Aluminium	n.a.	1.50 (0.009)	0.02 (0.02)	1.20 (0.06)
Boron	n.a.	1.30 (<0.05)	0.20 (<0.05)	0.80 (<0.05)
Mercury	n.a.	-	-	-
Lead	n.a.	0.07 (<0.0005)	-	-
Cadmium	n.a.	-	-	-
Cobalt	n.a.	0.01 (<0.0001)	0.03 (<0.0001)	0.02 (0.002)
Nickel	n.a.	0.02 (0.0006)	0.08 (0.0005)	0.05 (0.01)
Chromium	n.a.	0.006 (<0.0003)	-	0.0007 (0.0004)
Copper	n.a.	0.09 (0.0024)	0.03 (0.01)	0.009 (0.02)
Tin	n.a.	0.007 (<0.0003)	0.0002 (<0.0003)	-
Vanadium	n.a.	-	-	0.003 (<0.02)
Zinc	n.a.	2.50 (0.01)	0.70 (0.004)	-
Antimony	n.a.	0.10 (0.0012)	0.20 (<0.0002)	0.008 (0.002)
Arsenic	n.a.	-	-	-
Lithium	n.a.	-	4.10 (<0.04)	32 (0.2)
Molybdenum	n.a.	0.50 (0.01)	0.01 (0.0015)	0.03 (0.002)
Manganese	n.a.	0.09 (0.003)	0.14 (0.008)	0.11 (0.01)
Ions analysed; values presented are background corrected (mg L^{-1})				
Fluoride	n.a.	12.0	3.50	44
Chloride	n.a.	110	120	34
Bromide	n.a.	1.4	1.20	4.0

(-) indicate that the analysed compound was below the detection limit
Number shown with a (<) in front of the number are below the detection limit,
*no sprinklers active, not applicable (n.a.)

Table A4. Metal and ion content of water samples (samples taken end of test). Numbers in brackets indicate the error of the measurement obtained from water sampling before each test. All tabulated values have been rounded. Measurement uncertainty ± 10%

Compound	Reference test	ICEV	BEV	Battery
Concentration (mg L^{-1})				
Aluminium	0.01 (0.009)	0.30 (0.009)	1.40 (0.02)	6.40 (0.06)
Boron	0.80 (<0.05)	0.20 (<0.05)	0.70 (<0.05)	1.80 (<0.05)
Mercury	-	-	-	-
Lead	-	0.006 (<0.0001)	-	-
Cadmium	-	-	-	-
Cobalt	0.002 (<0.0001)	0.06 (<0.0001)	0.0002 (<0.0001)	-
Nickel	0.0008 (0.0006)	0.02 (0.0006)	-	-
Chromium	0.0008 (<0.0003)	0.0004 (<0.0003)	0.01 (<0.0003)	0.0004 (0.0004)
Copper	0.004 (0.002)	0.05 (0.002)	0.003 (0.01)	0.002 (0.02)
Tin	0.0003 (<0.0003)	0.002 (<0.0003)	-	-
Vanadium	0.006 (<0.002)	-	0.006 (<0.002)	0.004 (<0.02)
Zinc	0.004 (0.01)	4.60 (0.01)	-	-
Antimony	0.24 (0.0012)	0.12 (0.0012)	0.04 (<0.0002)	0.02 (0.002)
Arsenic	-	-	-	-
Lithium	0.25 (<0.04)	0.04 (<0.04)	30 (<0.04)	110 (0.2)
Molybdenum	0.09 (0.01)	0.004 (0.01)	0.14 (0.002)	0.11 (0.002)
Manganese	-	-	-	-
Ions analysed; values presented are background corrected				
Fluoride	2.30	7.60	19	70
Chloride	1300	250	140	53
Bromide	38	7.0	5.80	9

(-) indicate that the analysed compound was below the detection limit
Numbers shown with a (<) in front of the number are below the detection limit.

Appendix 6: PAH, VOC and PFAS

Table A5. Total amount of particulate-bound PAHs on each of the analysed filters, sampling combustion gas. LOQ = 0.1 µg

PAH	Blank	Ref. test	ICEV	BEV	Battery
			(µg per filter)		
Naphthalene	-	-	0.2	-	-
Acenaphthylene	-	-	-	-	-
Acenaphthene	-	-	-	-	-
Fluorene	0.2	-	-	-	0.1
Phenanthrene	-	1.3	-	-	-
Anthracene	-	1.0	-	-	0.1
Fluoranthene	-	4.4	4.0	2.8	-
Pyrene	-	4.7	4.5	3.1	-
Benzo [a] anthracene	-	3.1	4.4	2.9	-
Chrysene	-	5.3	6.1	5.0	0.1
Benzo [b,j] fluoranthene	0.1	9.7	10.9	6.5	-
Benzo [k] fluoranthene	0.1	4.3	5.4	3.7	-
Benzo [a] pyrene	-	3.6	6.5	3.8	-
Indeno [1,2,3-c, d] pyrene	-	8.1	11	5.8	-
Dibenz[ah]anthracene	-	-	-	-	-
Benzo[g, h, i]perylene	0.1	7.9	11	5.8	-
Sum of 16 PAHs	**0.5**	**53**	**64**	**40**	**0.3**
(–) below detection limit					

Table A6. PAH detected in water samples. All analysed PAHs are presented in Table A5. LOQ = 0.5 µg L^{-1}

PAH	ICEV T	ICEV E	BEV T	BEV E	Battery T	Battery E
			($\mu g\ L^{-1}$)			
Naphthalene	1.8	1.8	-	-	-	-
Acenaphthylene	1.0	0.8	-	-	-	-
Acenaphthene	5.0	8.5	1.8	-	-	-
Fluorene	1.3	-	0.8	-	-	-
Phenanthrene	1.7	0.6	-	-	-	-
Anthracene	1.5	1.0	-	-	-	-
Sum of 16 PAHs	**12**	**13**	**< 2.6**	**-**	**-**	**-**
(–) below detection limit **T** – time resolved testing (time 0 – 30 min) **E** – end of test						

Table A7. Concentration of VOCs for water sample taken after the ICEV test, the remaining water samples (reference, BEV and battery fire test) were free of VOCs. LOQ = 10 µg L^{-1}

Compound	CAS	ICEV end of test
		(µg L^{-1})
Cyclopentanone	120-92-3	320
2-Propanone, 1-(1-methylethoxy)-	42781-12-4	578
Benzonitrile	100-47-0	128
Phenol	108-95-2	367
Ethanone, 2,2-dihydroxy-1-phenyl-	1075-06-5	94
2-Acetyl-2-methyltetrahydrofuran	32318-87-9	88
Glycidyl isopropyl ether	4016-14-2	89
m-Isopropylphenol	618-45-1	65
2-Propenenitrile, 3-phenyl-	1885-38-7	68
Caprolactam	105-60-2	391
Phenol, p-tert-butyl-	98-54-4	46
Benzenebutanenitrile	2046-18-6	98
Biphenol A	1980-05-07	221
unknown		23
Sum of compounds		**2577**

Table A8. Concentration and targeted PFAS for water sample taken after the tests. Measurement uncertainty ~ 30%

Compound	LOQ	Blank 1	Blank 2	Blank 3	Ref	ICEV	BEV	Battery
				ng L^{-1} (ppt)				
PFBA	50	-	-	-	-	-	-	113
PFPeA	50	-	-	-	68	137	-	101
PFBS	10	-	-	-	97	-	137	2252
PFHxA	10	71	60	62	113	215	-	268
PFPeS	10	-	-	-	-	-	-	-
PFHpA	10	12	-	-	-	24	-	66
PFHxS	10	-	-	-	-	-	-	64
PFOA	10	-	-	-	12	19	12	139
6:2 FTS	10	-	32	-	1019	447	47	1313
PFHpS	10	-	-	-	-	-	-	-
PFNA	10	-	-	-	-	-	-	-
PFOS	10	-	-	-	-	-	-	348
PFDA	10	-	-	-	-	-	-	-
PFNS	10	-	-	-	-	-	-	-
PFUdA	10	-	-	-	-	-	-	-
PFDS	10	-	-	-	-	-	-	-
PFDoDA	10	-	-	-	-	-	-	-
PFUdS	10	-	-	-	-	-	-	-
PFTrDA	10	-	-	-	-	-	-	-
PFDoDS	10	-	-	-	-	-	-	-
PFTeDA	10	-	-	-	-	-	-	-
PFTrDS	10	-	-	-	-	14	-	-
Sum PFAS	-	83	92	62	1310	856	196	4664

Through our international collaboration programmes with academia, industry, and the public sector, we ensure the competitiveness of the Swedish business community on an international level and contribute to a sustainable society. Our 2,800 employees support and promote all manner of innovative processes, and our roughly 100 testbeds and demonstration facilities are instrumental in developing the future-proofing of products, technologies, and services. RISE Research Institutes of Sweden is fully owned by the Swedish state.

I internationell samverkan med akademi, näringsliv och offentlig sektor bidrar vi till ett konkurrenskraftigt näringsliv och ett hållbart samhälle. RISE 2 800 medarbetare driver och stöder alla typer av innovationsprocesser. Vi erbjuder ett 100-tal test- och demonstrationsmiljöer för framtidssäkra produkter, tekniker och tjänster. RISE Research Institutes of Sweden ägs av svenska staten.

RISE Research Institutes of Sweden AB Box 857, 501 15 BORÅS, SWEDEN Telephone: +46 10-516 50 00 E-mail: info@ri.se, Internet: www.ri.se	Fire Safe Transport RISE Report 2023:22 ISBN: 978-91-89757-65-3